CONSEJO SUPERIOR DE INVESTIGACIONES CIENTÍFICAS

INSTITUTO DE CIENCIA DE MATERIALES DE MADRID (ICMM)

Quantum state transfer mediated by topological edge states

Gloria Platero

Materials Science Institute of Madrid (ICMM-CSIC)

modern trends in condensed matter physics

Capri Spring School

Outline

- Quantum information transfer through quantum dot arrays: introduction
- Floquet engineering : QD arrays as Quantum Simulators of 1D Topological Insulators
- Quantum information transfer in 1D topological insulators: the role of edge states
- Speeding up the transfer of quantum information: topological domain walls
- Qubits coupled to each other through edge states: coherent operation of multi-qubit states

Semiconductor quantum dots as a platform for the quantum computer

Loss and Divicenzo, PRA 1998

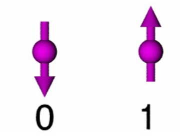

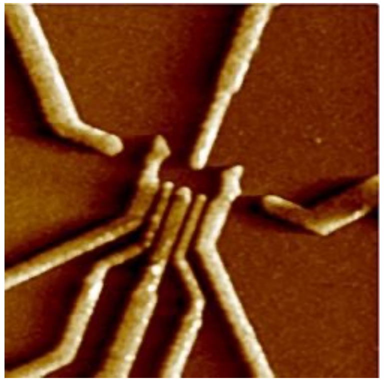

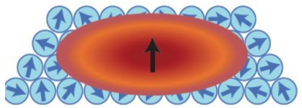

GaAs: strong hyperfine interaction: source of spin decoherence and relaxation

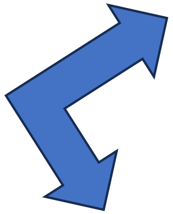

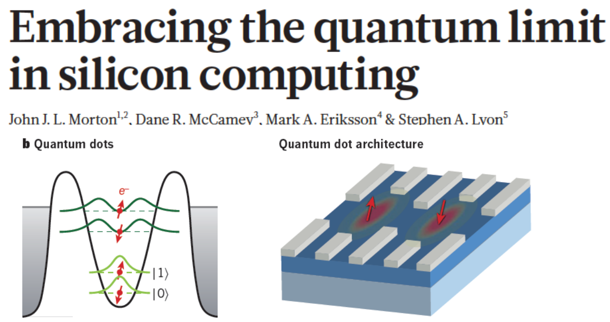

J. Morton et al., Nature, 2011

The germanium quantum information route

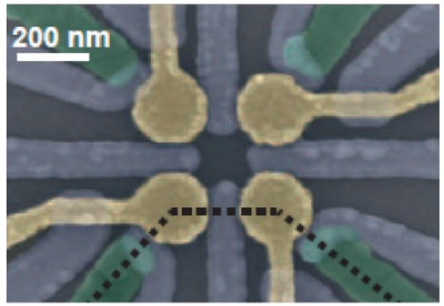

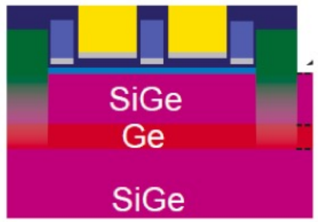

G. Scappucci et al., Nature Rev. Mat, 2021

Hole spin qubits

Spin Exchange: two qubits operations

Coherent spin rotations: one qubit operations

Koppens et al. Nature 2006

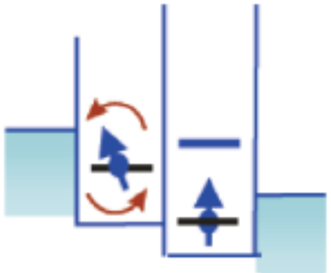

B_{AC}

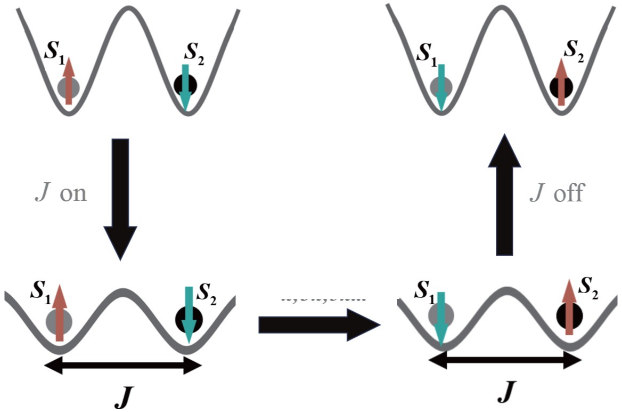

Petta et al., Science 2005

Quantum Links: Communication between distant sites in a quantum chip

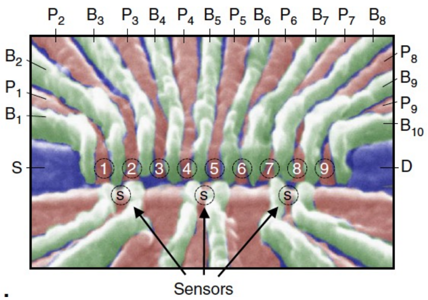

Zajac et al., Phys Rev App (2016)

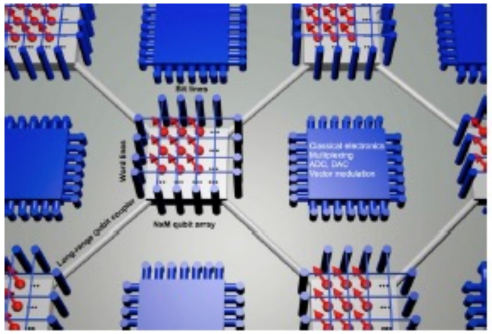

A key challenge: maintain gate fidelity as the system scales: Modular architectures connecting small, high-coherence units through quantum links

Fast and High-fidelity transfer protocol: robust against different noise sources

Experimentally feasible driving pulses: few control pulses avoiding fan-out problem

Long Range Quantum Transfer in QD arrays

M. Busl et al., Nature Nanotech, 8, 262 (2013)

R. Sánchez et al., PRL 112, 176803 (2014)

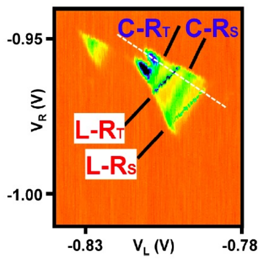

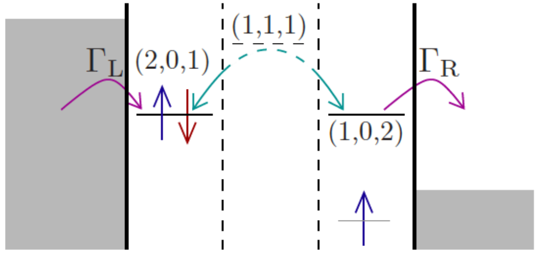

$$|LR\rangle = \frac{1}{\sqrt{2}}\left(|\uparrow\downarrow,0,\uparrow\rangle - |\uparrow,0,\uparrow\downarrow\rangle\right)$$

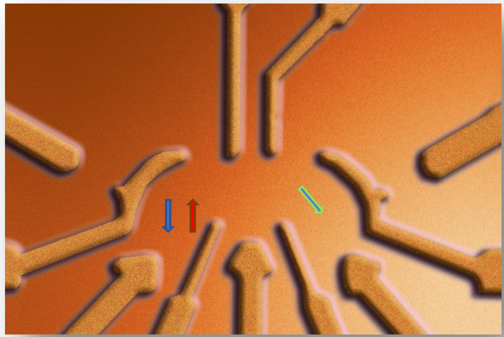

NRC, Ottawa
A. Sachrajda

As an electron tunnels from one extreme to the other a spin state is transferred in the opposite direction

- Long range photo-assisted tunneling

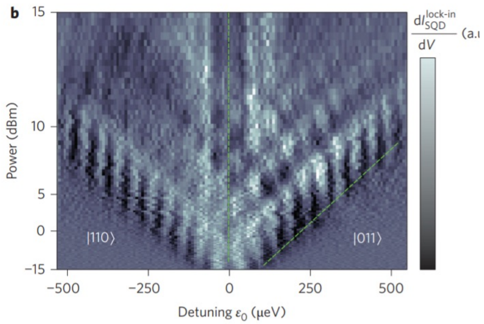

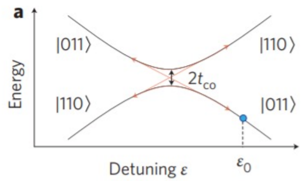

F. Braakman et al.
Nature Nanotech
2013

J. Picó-Cortés, F. Gallego-Marcos and G. P., PRB, 99, 155421 (2019)
P. Stano et al., PRB 2015
F. Gallego et al., JAP 2015
F. Gallego et al., PRB 2017

Long Range Quantum Transfer in QD arrays

M. Busl et al., Nature Nanotech, 8, 262 (2013)

R. Sánchez et al., PRL 112, 176803 (2014)

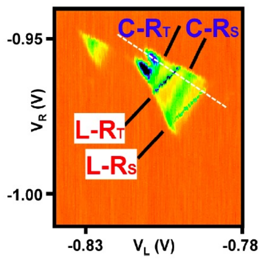

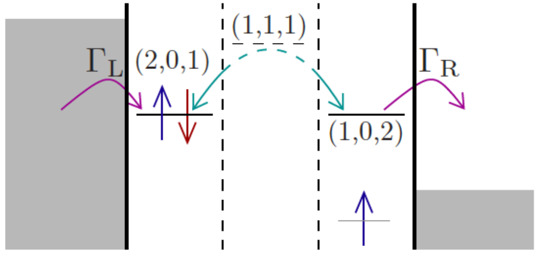

$$\left|LR\right\rangle = \frac{1}{\sqrt{2}}\left(\left|\uparrow\downarrow,0,\uparrow\right\rangle - \left|\uparrow,0,\uparrow\downarrow\right\rangle\right)$$

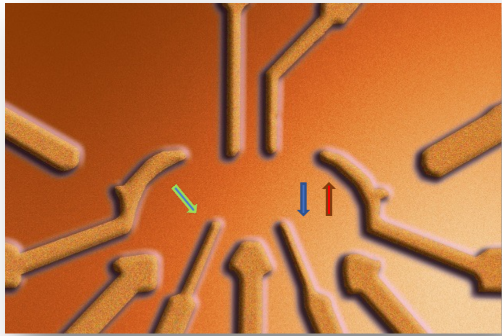

NRC, Ottawa
A. Sachrajda

As an electron tunnels from one extreme to the other a spin state is transferred in the opposite direction

- Long range photo-assisted tunneling

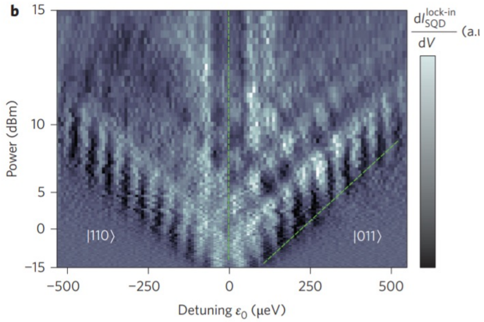

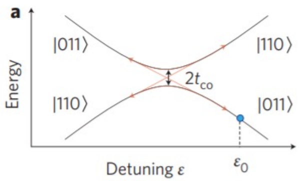

F. Braakman et al.
Nature Nanotech
2013

J. Picó-Cortés, F. Gallego-Marcos and G. P., PRB, 99, 155421 (2019)
P. Stano et al., PRB 2015
F. Gallego et al., JAP 2015
F. Gallego et al., PRB 2017

Long range quantum transfer in QD arrays

Coherent Transfer by Adiabatic Passage (CTAP)

$$\Omega_{12}(t) = \Omega^{\max} \exp\left[-\left(t - \frac{t_{\max}+\sigma}{2}\right)^2 / (2\sigma^2)\right]$$

$$\Omega_{23}(t) = \Omega^{\max} \exp\left[-\left(t - \frac{t_{\max}-\sigma}{2}\right)^2 / (2\sigma^2)\right]$$

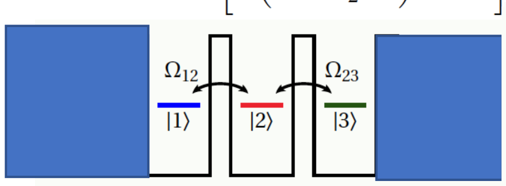

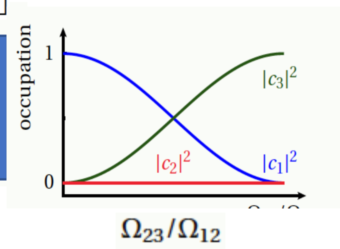

Dark State

$$\varepsilon = 0$$

$$|\varphi\rangle = |D_0\rangle = \cos\theta|1\rangle - \sin\theta|3\rangle$$

$$\theta = \arctan(\Omega_{12}/\Omega_{23})$$

Spin conserving tunneling

A. Greentree et al., PRB, 70, 235317 (2004)

Coherent Trapping of Atomic Populations in Optics

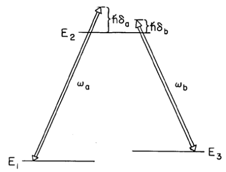

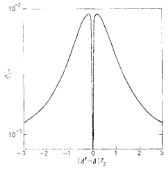

E. Arimondo et al., Lettere al Nuovo Cimento , 1976

C. Beenakker, EPL 2006

Coherent transport of spin by adiabatic passage in quantum dot arrays, MJ Gullans, J. Petta, PRB 2020

Long range quantum transfer in QD arrays

Coherent Transfer by Adiabatic Passage (CTAP)

$$\Omega_{12}(t) = \Omega^{\max} \exp\left[-\left(t - \frac{t_{\max}+\sigma}{2}\right)^2 / (2\sigma^2)\right]$$

$$\Omega_{23}(t) = \Omega^{\max} \exp\left[-\left(t - \frac{t_{\max}-\sigma}{2}\right)^2 / (2\sigma^2)\right]$$

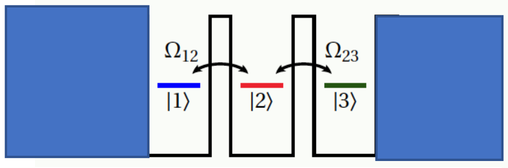

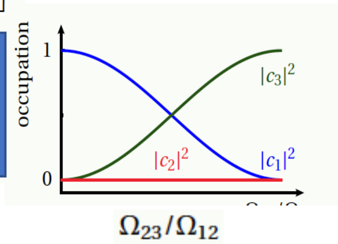

Dark State

$\varepsilon = 0$

$$|\varphi\rangle = |D_0\rangle = \cos\theta|1\rangle - \sin\theta|3\rangle$$

$$\theta = \arctan(\Omega_{12}/\Omega_{23})$$

Spin conserving tunneling

A. Greentree et al., PRB, 70, 235317 (2004)

Dark State for holes

$$H_{SOI} \Rightarrow \boxed{\sum_i \left[-\tau_{F,i}\left(c^\dagger_{i\uparrow}c_{i+1\downarrow} - c^\dagger_{i\downarrow}c_{i+1\uparrow}\right) + \text{h. c.}\right]}$$

Proportional **spin-flip** and **spin-conserving** tunneling rates

$$\boxed{\tau_{F,i}(t)/\tau_{N,i}(t) = x_{\text{SOC}}}$$

$$\boxed{\tan\theta \equiv \tau_{N,2}/\tau_{N,1}}$$

$$|\text{DS}_1\rangle = -\sin\theta|\uparrow,0,0\rangle + \frac{\cos\theta}{x^2_{\text{SOC}}+1}\boxed{\left[(x^2_{\text{SOC}}-1)\,|0,0,\uparrow\rangle\right.} + \boxed{\left.2x_{\text{SOC}}\,|0,0,\downarrow\rangle\right]}$$

A. Bogan et al., PRL, 2018, ; G. Burkard et al., PRR 2021;
D. Fernández-Fernández et al., Quantum (2024)

Quantum transfer in QD arrays

Shortcuts to Adiabaticity (STA)
versatil ways to speed up adiabatic passages
D. Guéry-Odelin et al., RMP., 91, 045001, 2019

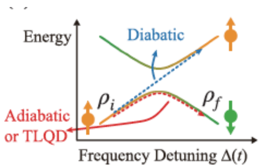

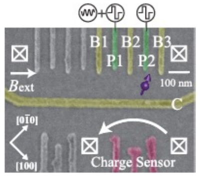

Xiao-Fei Liu, Phys Rev. Lett., 132, 027002 (2024)
D. Fernández-Fernández et al., Phys Rev Appl., 18,054090 (2022)

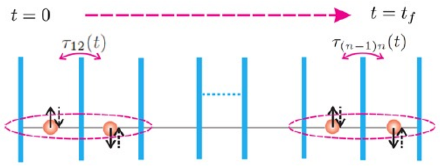

Y. Ban, et al., Nanotech., 29, 505201 (2018)

Y. Ban et al., Adv. Quantum Tech., 1900048 (2019)

Flying spin qubits in quantum dot arrays driven by spin-orbit interaction,
D. Fernández-Fernández, Y. Ban and G. Platero, Quantum 8, 1533 (2024)

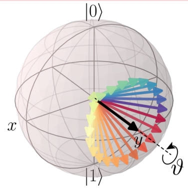

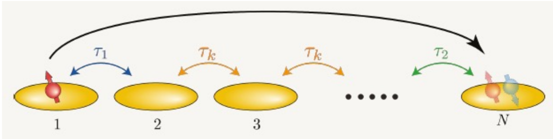

Hybrid Systems: Cavity-QDs

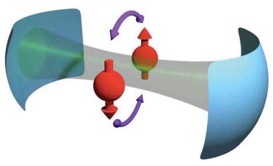

Mi et al., Nature 555, 599 (2018)
Samkharadze et al., Science, 359, 1123 (2018)

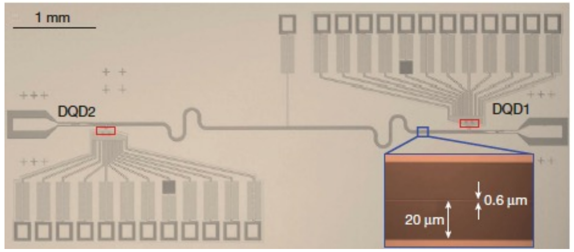

Borjans et al., Nature 577, 195 (2020)

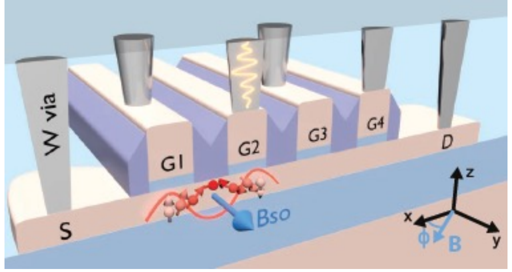

Cecile Yu et al., Nature Nanotech., 18, 741 (2023)

Quantum transfer in QD arrays

single-electron Conveyor-Mode QuBus in Si/SiGe Propagating sinusoidal potential

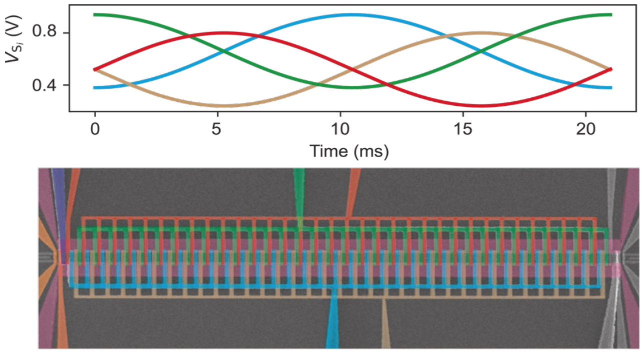

R. Xue, et al., Nat. Commun. , 2024

S. Bosco et al., PRX, 2024
D. Fernández-Fernández et al., arXiv:2508.08394

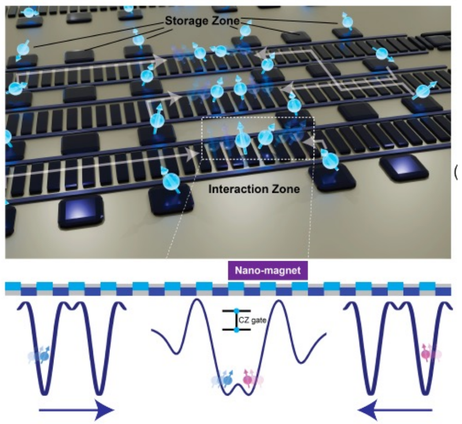

- M. de Smet et al., Nature Nanotech. 2025

Bucket Brigade

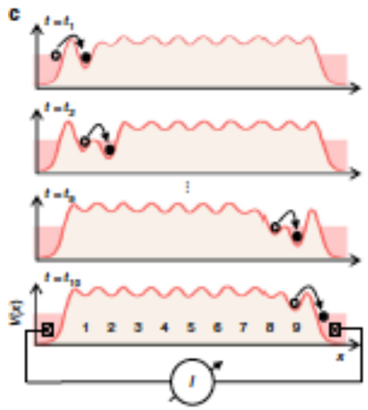

A.R. Mills et al., Nat Comm, 2019

Nakajima et. al., Nat. Comm. 2018

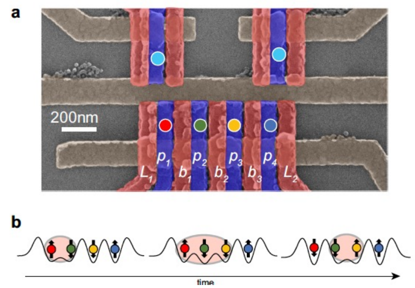

Y. P. Kandel et al.,
Nature Comm. 2021

Quantum state transfer by topological edge states

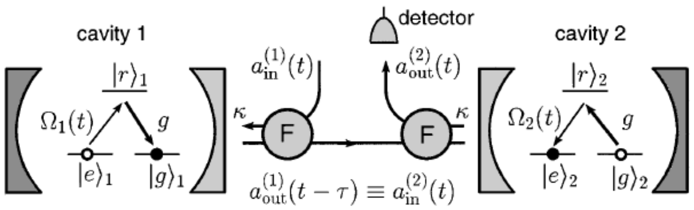

J. I. Cirac et al., PRL 97

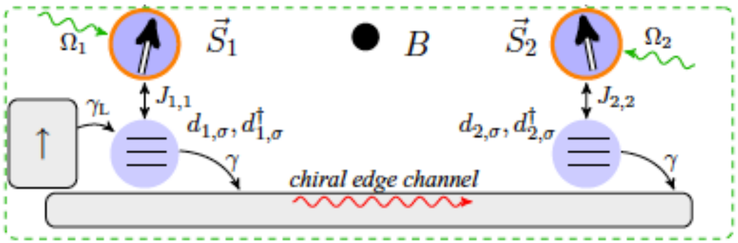

Mesoscopic One-Way Channels for Quantum State Transfer via the Quantum Hall Effect
Stace et al., PRL, 2004

Long-distance entanglement of spin qubits via quantum Hall edge states, G. Yang et al., PRB 2016

Long-range entanglement generation between electronic spins, M. Benito et al., PRB 2016

Entangling Nuclear Spins in Distant Quantum Dots via an Electron Bus, M. Bello et al., Phys. Rev. Applied, 2022.

Quantum state transfer by topological edge states

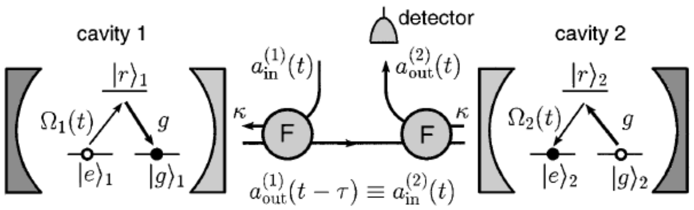

J. I. Cirac et al., PRL 97

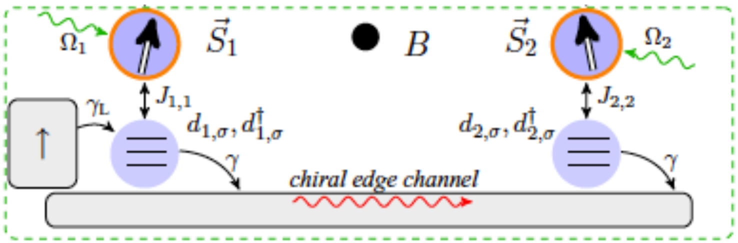

Mesoscopic One-Way Channels for Quantum State Transfer via the Quantum Hall Effect
Stace et al., PRL, 2004

Long-distance entanglement of spin qubits via quantum Hall edge states, G. Yang et al., PRB 2016

Long-range entanglement generation between electronic spins, M. Benito et al., PRB 2016

Entangling Nuclear Spins in Distant Quantum Dots via an Electron Bus, M. Bello et al., Phys. Rev. Applied, 2022.

Is it posible to simulate a 1D Topological Insulator in a semiconductor QD array?

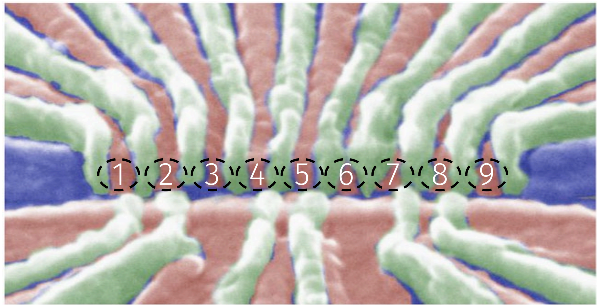

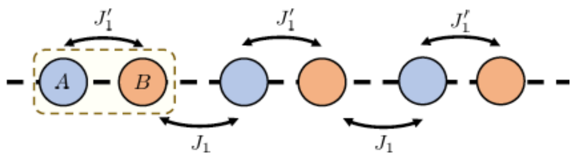

QDs as Quantum Simulators

Quantum Simulation of the Fermi-Hubbard model using QD arrays,
T. Henggens et al., Nature, 2017

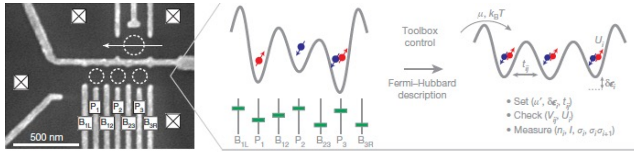

A Tunable Kondo Effect in Quantum Dot
S. Cronnenwelt et al., Science 98

Kondo effect and SO coupling in Graphene QDs,
A. Kurzman et al., Nat. Comm., 2021

Proposal for Detection of the 0′ and π′ Phases in
Quantum dot Josepshon Junctions M. Lee et al., PRL 2022

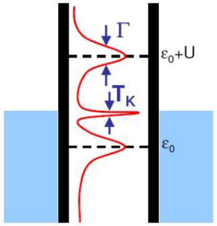

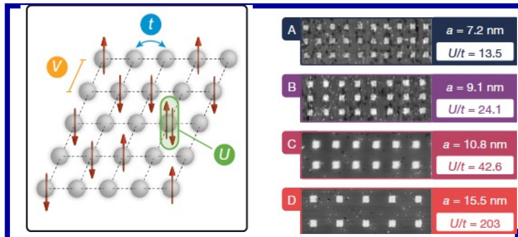

Large scale analog quantum simulation
using atom dot arrays

M.B. Donnelly et al., Nature 2026

Dynamical control of correlated
states in a square quantum dot
C. Crefield and GPlatero, PRB 2002

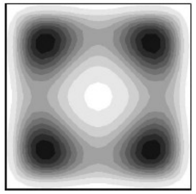

Nagaoka ferromagnetism
observed in a QD plaquette,
JP Dehollais et al., Nature 2020

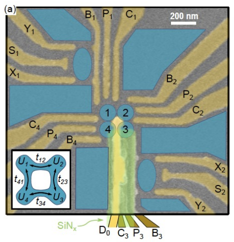

Exciton Transport in a Germanium
Quantum Dot Ladder

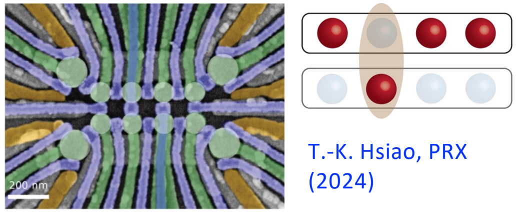

T.-K. Hsiao, PRX
(2024)

Site-resolved magnon and triplon dynamics on a
programmable quantum dot spin ladder

Pablo Cova Fariña et al., arXiv:2506.08663v1

Engineering topological states in
atom-based
semiconductor quantum dots

M. Kiczynski et al.
Nature, June 2022

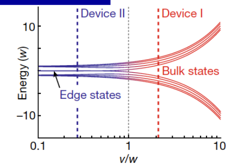

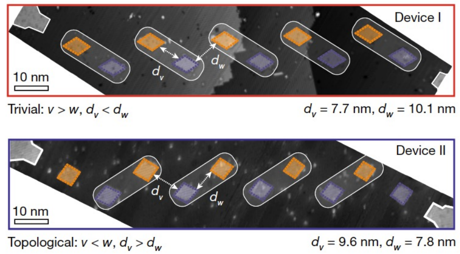

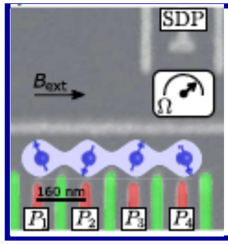

Quantum Simulation of
Antiferromagnetic Heisenberg Chain
with Gate defined QDs,
PRX, C.J. van Diepen et al., 2021

Quantum simulation of 1D Topological Insulators

superconducting qubit chains,
Feng Mei et al., Phys Rev A, 2018

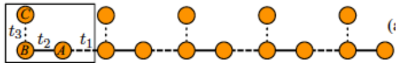

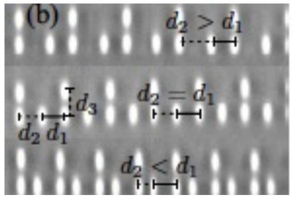

Edge states in SSH-Stub photonic lattices

G. Cáceres-Aracena et al, PRR. 4, 013185 (2022)

Topological microlaser array on a hybrid silicon platform

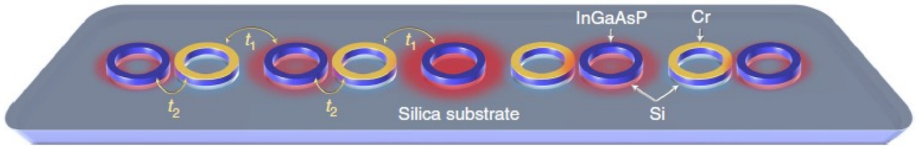

Zhao et al., Nature Comm, 2018

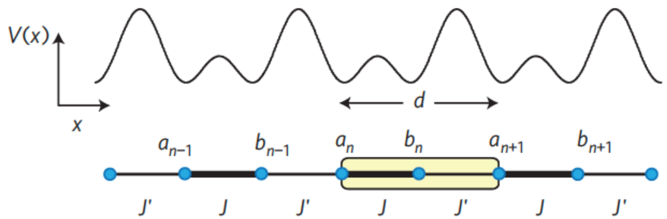

Cold atoms, N. Atala et al., Nature Phys., 2013

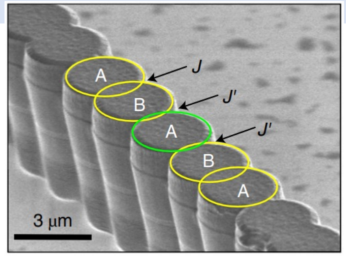

N. Pernet et al., Nat. Phys. **18**, 678 (2022)

Waveguide arrays

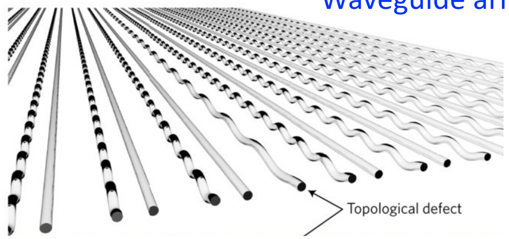

S. Weimann et al., Nat. Mater. **16**, 433 (2017)

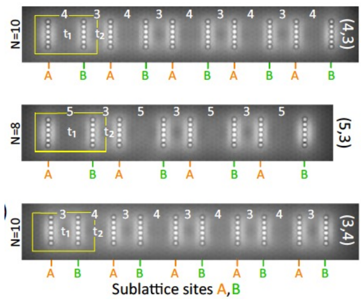

In adatoms

Pan et al.,
PRB, **105**, 125418 (2022)

Topological states in dimerized quantum-dot chains
created by atom manipulation

QD arrays as simulators of a 1D Topological Insulator

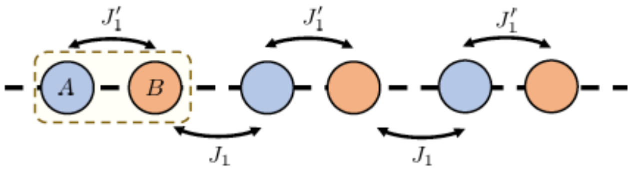

Dimer chain (SSH model)

$$H = -J_1' \sum_{i=1,\sigma}^{M} c^\dagger_{2i\sigma} c_{2i-1\sigma} - J_1 \sum_{i=1,\sigma}^{M-1} c^\dagger_{2i+1\sigma} c_{2i\sigma} + \text{h.c.}$$

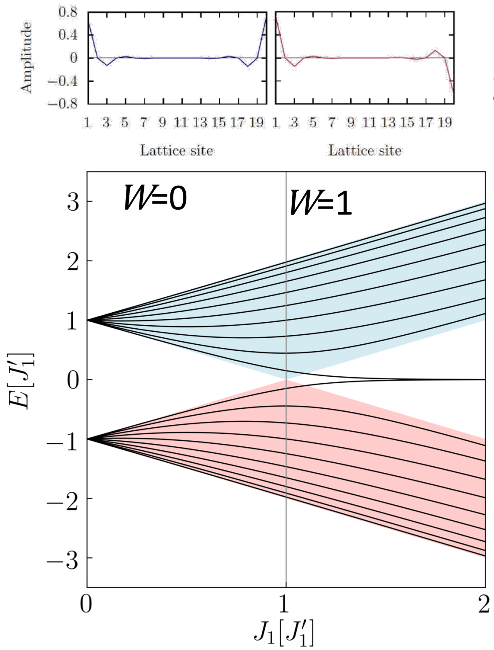

BDI class in the Altland-Zirnbauer classification

$$\mathcal{C}\mathcal{H}(k)\mathcal{C}^{-1} = -\mathcal{H}(-k)$$
$$\mathcal{T}\mathcal{H}(k)\mathcal{T}^{-1} = \mathcal{H}(-k)$$
$$\mathcal{X}\mathcal{H}(k)\mathcal{X}^{-1} = -\mathcal{H}(k)$$

$$\mathcal{W} = \frac{1}{2\pi}\int \langle u_{\alpha,k}|i\partial_k|u_{\alpha,k}\rangle dk$$

Berry's phase picked up by a particle moving accross the Brillouin zone.

The level splitting decays exponentially with the number of atoms

Beatriz Pérez-González et al., PRB,99,035146 (2019)

QD arrays as simulators of a 1D Topological Insulator

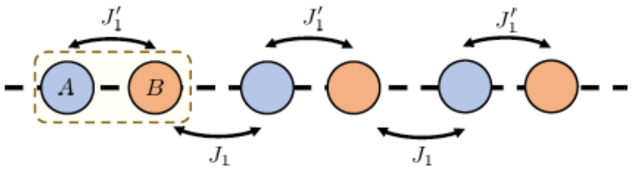

Dimer chain (SSH model)

$$H = -J_1' \sum_{i=1,\sigma}^{M} c^\dagger_{2i\sigma} c_{2i-1\sigma} - J_1 \sum_{i=1,\sigma}^{M-1} c^\dagger_{2i+1\sigma} c_{2i\sigma} + \text{h.c.}$$

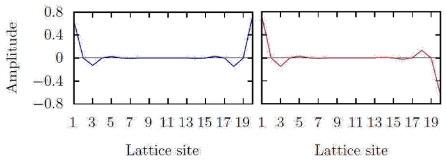

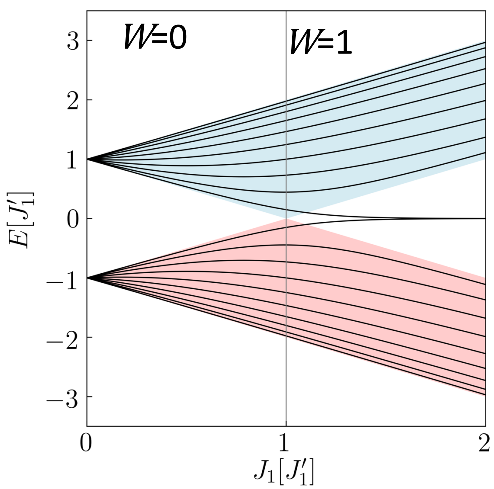

BDI class in the Altland-Zirnbauer classification

$$\mathcal{C}\mathcal{H}(k)\mathcal{C}^{-1} = -\mathcal{H}(-k)$$
$$\mathcal{T}\mathcal{H}(k)\mathcal{T}^{-1} = \mathcal{H}(-k)$$
$$\mathcal{X}\mathcal{H}(k)\mathcal{X}^{-1} = -\mathcal{H}(k)$$

$$\mathcal{W} = \frac{1}{2\pi}\int \langle u_{\alpha,k}|i\partial_k|u_{\alpha,k}\rangle dk$$

Berry's phase picked up by a particle moving accross the Brillouin zone.

The level splitting decays exponentially with the number of atoms

Beatriz Pérez-González et al., PRB,99,035146 (2019)

even-neighbor hoppings

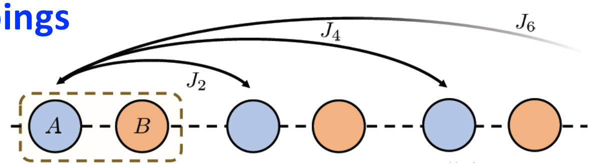

broken chiral symmetry

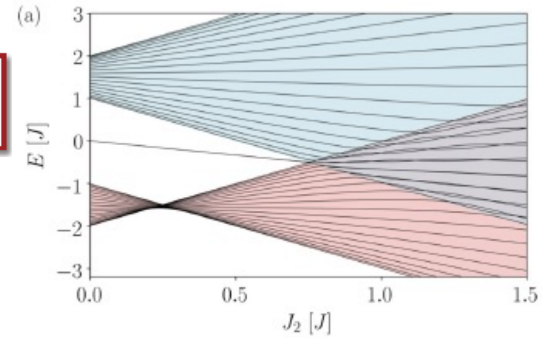

odd-neighbor hoppings

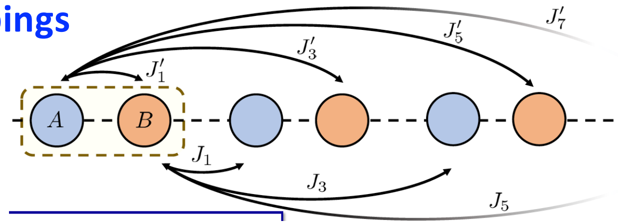

✓ chiral symmetry $\mathcal{W} = 0, 1, 2, 3, \ldots$

first and third neighbors

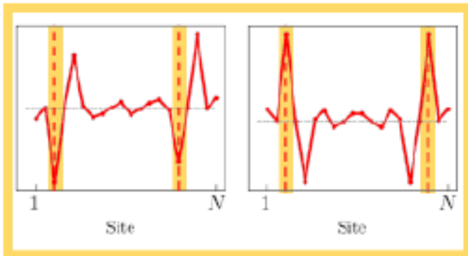

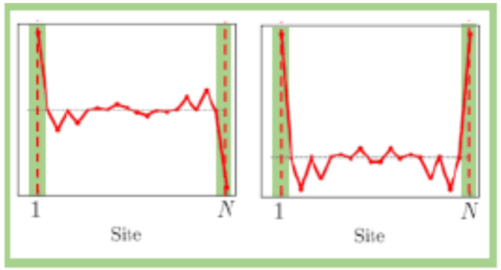

Floquet Engineering

Floquet engineering of quantum materials: **modify the properties** of the system through the interaction with **classical light** T. Oka and S. Kitamura, Ann. Rev. Cond. Matt. Phys. **10**, pp 387-408 (2019)

Floquet theory: solve the dynamics of time-periodic systems A. Eckardt, Rev. Mod. Phys. **89**, 011004 (2017)

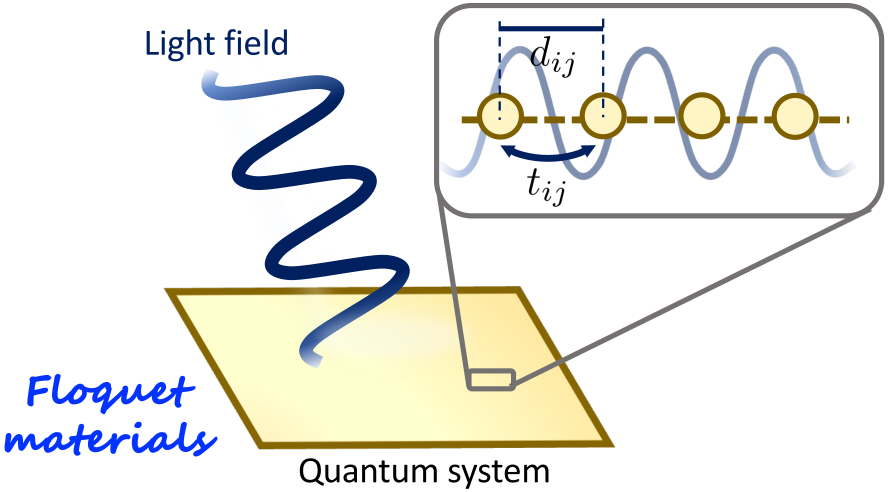

$$i\partial_t|\psi_n(t)\rangle = H_{\text{tot}}(t)|\psi_n(t)\rangle$$

$$|\psi_n(t)\rangle = |\phi_n(t)\rangle e^{-i\varepsilon_n t}$$

Floquet modes: $|\phi_n(t)\rangle = |\phi_n(t+T)\rangle$

Quasienergies: $\varepsilon_n \to \varepsilon_{nm} = \varepsilon_n + m\omega$

$$\underbrace{[H(t) - i\partial_t]}_{\mathcal{F}\,\equiv\,\text{Floquet operator}}|\phi_{nm}(t)\rangle = \varepsilon_{nm}|\phi_{nm}(t)\rangle$$

quasienergies are conserved quantities and take up the role of the energy in time-independent systems

Floquet Engineering

Floquet engineering of quantum materials: **modify the properties** of the system through the interaction with **classical light** T. Oka and S. Kitamura, Ann. Rev. Cond. Matt. Phys. **10**, pp 387-408 (2019)

Floquet theory: solve the dynamics of time-periodic systems A. Eckardt, Rev. Mod. Phys. **89**, 011004 (2017)

- **high-frequency regime:** $\omega \gg t_{ij}$

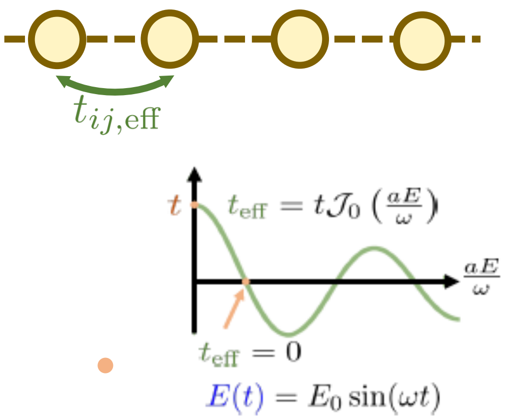

the system is governed by an **effective, time-independent Hamiltonian**

renormalized hopping amplitudes

Reported measurement of dynamical suppression of tunneling in optical lattices

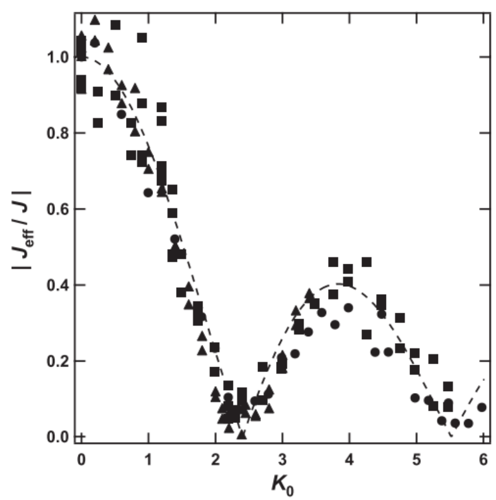

H. Lignier et al., Phys. Rev. Lett. **99**, 220403 (2007)

Driving with periodic AC fields

Photoassisted Tunneling (PAT) in quantum dots

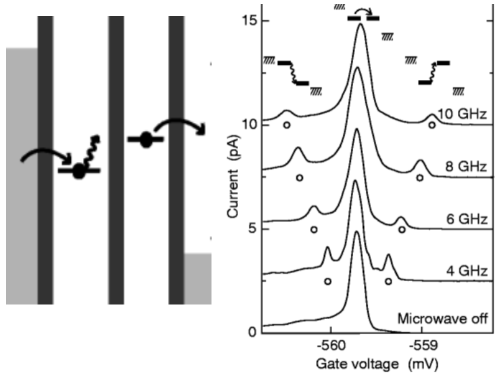

T. H. Oosterkamp et al., Nature 395, 873, 1998

Coherent destruction of tunnel,
P. Hänggi, PRL, 1991

Bonds renormalization

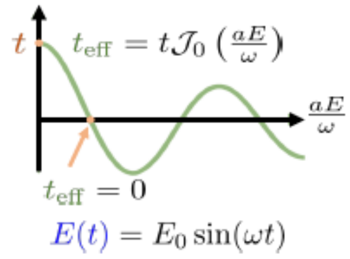

Tuning electronic and topological properties of lattices in driven systems.

Floquet-Bloch Theory for Hamiltonians periodic in both time and space

A. Gómez León and G.Platero, PRL,110, 200403 (2013)

Realization of an anomalous Floquet Topological Insulator with ultracold atoms
K. Wintersperger et al. Nature Phys., 2020

Driving protocol for a Floquet topological phase without static counterpart, A. Quelle et al., NJP, 2017

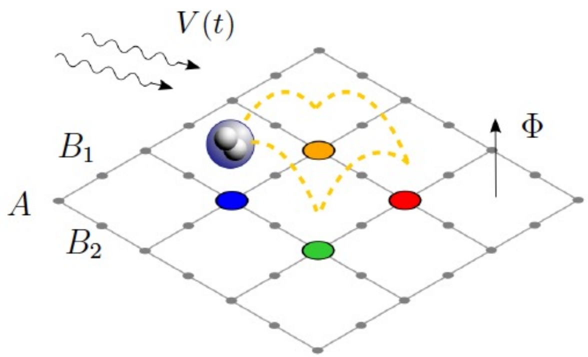

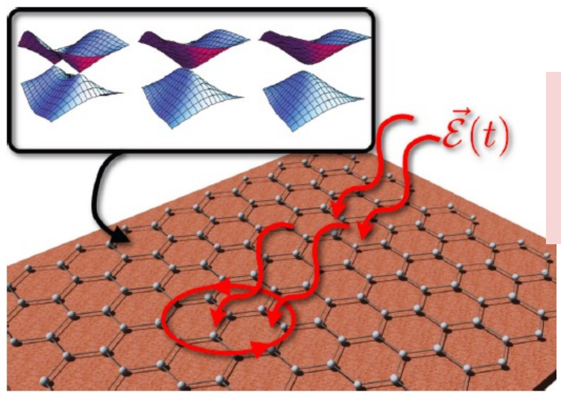

P. Delplace, A. Gómez León, G.Platero PRB 88, 245, 2013

M. Bello, C.E. Creffield and G. Platero, PRB, 95, 094303 (2017)

Driving with periodic AC fields

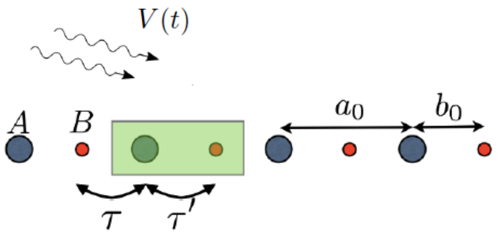

A. Gómez León and G.Platero, PRL,110, 200403 ,2013

$$H_{\rm tot}(t) = H_{\rm SSS} + H_{\rm driv}(t)$$

$$H_{\rm SSH} = \sum_j t_1' a_j^\dagger b_j + t_1 b_j^\dagger a_{j+1} + \text{h.c.}$$

$$H_{\rm driv}(t) = E(t) \sum_{i=1}^{N} x_i c_i^\dagger c_i$$

$$\omega \gg t, t'$$

$$\boxed{H_{\rm eff} = \sum_j \mathcal{J}_0\left(\frac{E_0 r'}{\omega}\right) t_1' a_j^\dagger b_j + \mathcal{J}_0\left(\frac{E_0(1-r')}{\omega}\right) t_1 b_j^\dagger a_{j+1} + \text{h.c.}}$$

Undriven Z=0

Undriven Z=1

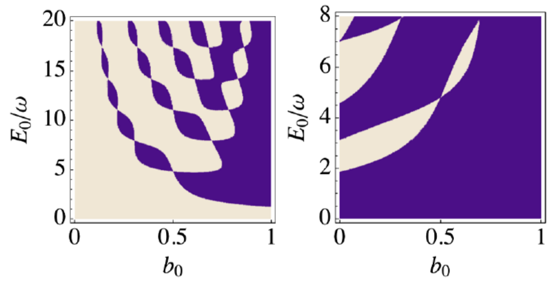

M. Bello et al., Scientific Rep, 6, 22562, 2016

M. Niklas et al., Nanotechnology, 2017

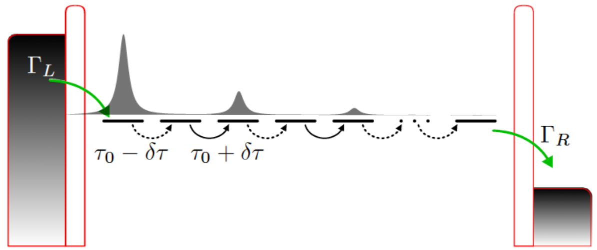

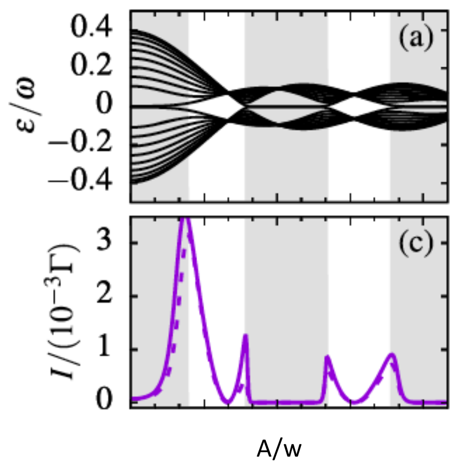

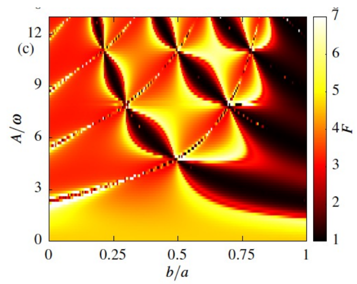

Fano factor

Driving with periodic AC fields

Photoassisted Tunneling (PAT) in quantum dots

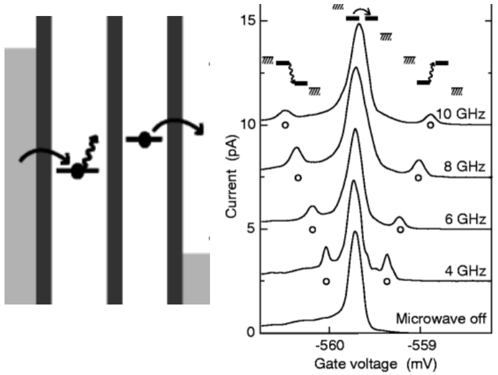

T. H. Oosterkamp et al., Nature 395, 873, 1998

Coherent destruction of tunnel,
P. Hänggi, PRL, 1991

Bonds renormalization

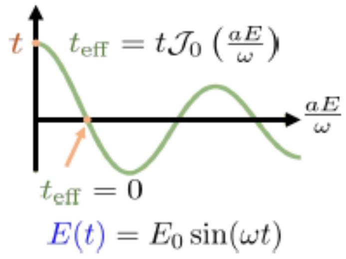

Tuning electronic and topological properties in driven systems

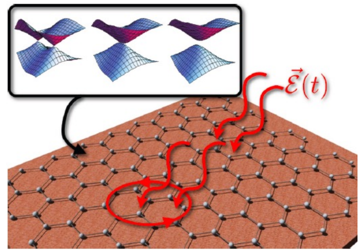

P. Delplace, A. Gómez León, GP
PRB 88, 245, 2013

Floquet topological insulators

M. Rudner and N. Lindner, Nature Rev. Phys., 2020

Quantum Floquet Engineering

Quantum Light +Quantum System

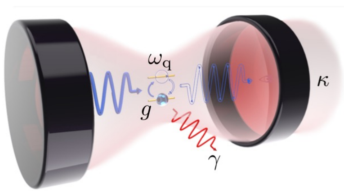

Feedback cavity- matter

$$E \propto d^\dagger + d$$

Light-matter correlations

B. Pérez-González et al., Quantum, 9, 1633 (2025)
B. Pérez-González et al., Comm. Physics, 7, 419 (2024)

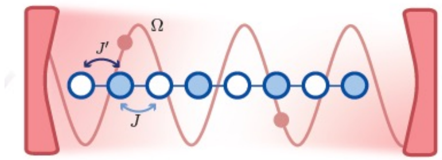

Simulation of the extended SSH Hamiltonian by an ac field

Floquet Engineering

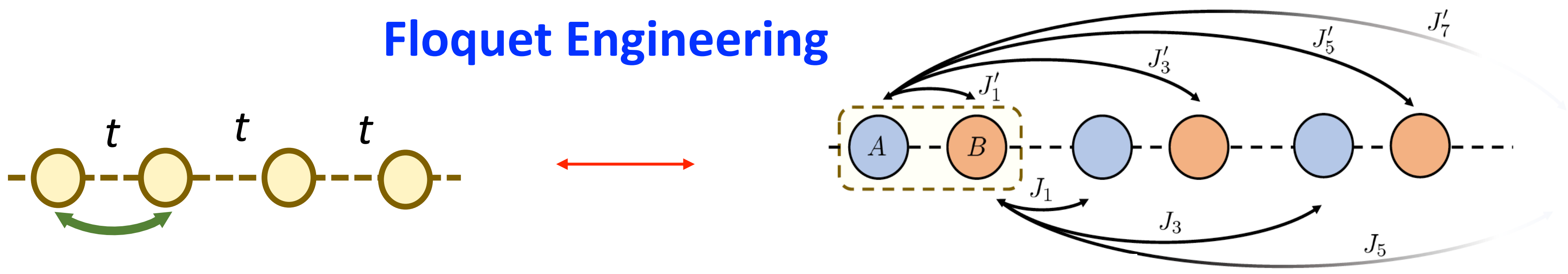

Simulation of the extended SSH Hamiltonian by an ac field

$$H(t) = \sum_{|i-j|<R} J_{ij} c_i^\dagger c_j + \sum_i A_i f(t) c_i^\dagger c_i$$

$$f(t) = \begin{cases} 1 & \text{if} \quad 0 \le t < T/2 \\ -1 & \text{if} \quad T/2 \le t < T \end{cases}$$

$$\omega \gg J_{ij}$$

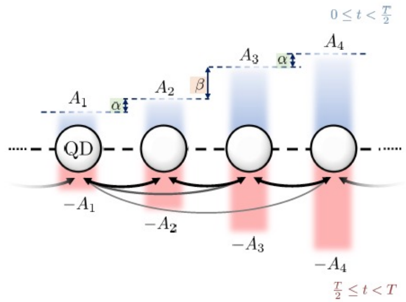

- Topological phases with a **large topological invariant** in the ac driven system

$$\boxed{H_{\text{eff}} = \sum_{|i-j|<R} \tilde{J}_{ij} c_i^\dagger c_j}$$

renormalized hopping amplitudes in terms of the field parameters

$$\tilde{J}_{ij} = J_{ij} \frac{i\omega}{\pi(A_i - A_j)} \left[e^{-i\pi \frac{A_i - A_j}{\omega}} - 1 \right]$$

- periodically spaced zeroes, located at

$$A_i - A_j = 2\omega q \quad (q = 0, 1, 2 \ldots)$$

- functions of the difference between on-site potentials

$$\tilde{t}_{12} \rightarrow A_1 - A_2 = \alpha \rightarrow \tilde{t}'$$
$$\tilde{t}_{23} \rightarrow A_2 - A_3 = \beta \rightarrow \tilde{t}$$
$$\tilde{t}_{34} \rightarrow A_3 - A_4 = \alpha \rightarrow \tilde{t}'$$
$$\tilde{t}_{45} \rightarrow A_4 - A_5 = \beta \rightarrow \tilde{t}$$

$$A_{2n} = n(\alpha + \beta)$$
$$A_{2n-1} = n(\alpha + \beta) - \alpha$$
$$n = 1, 2, 3, \ldots,$$

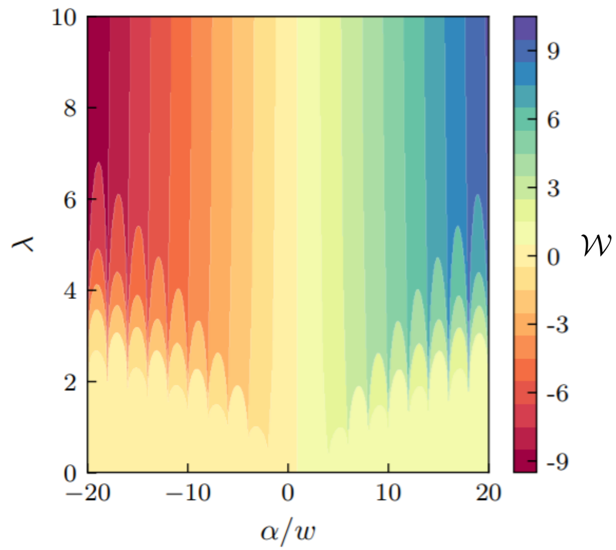

$|i-j|$=2*n*, *n*=1,2.... $\boxed{A_j - A_i = \alpha + \beta = 2\omega q}$ $\boxed{J_{i,\, i+2n}=0}$

B. Pérez-González et al., PRL,123,126401 (2019)

Simulation of the extended SSH Hamiltonian by an ac field

B. Pérez-González et al., PRL,123,126401 (2019)

dynamics of two particles with opposite spin loaded into the system $|\uparrow_1\downarrow_3\rangle$

Topological properties controlled through the tuning of the **driving parameters**

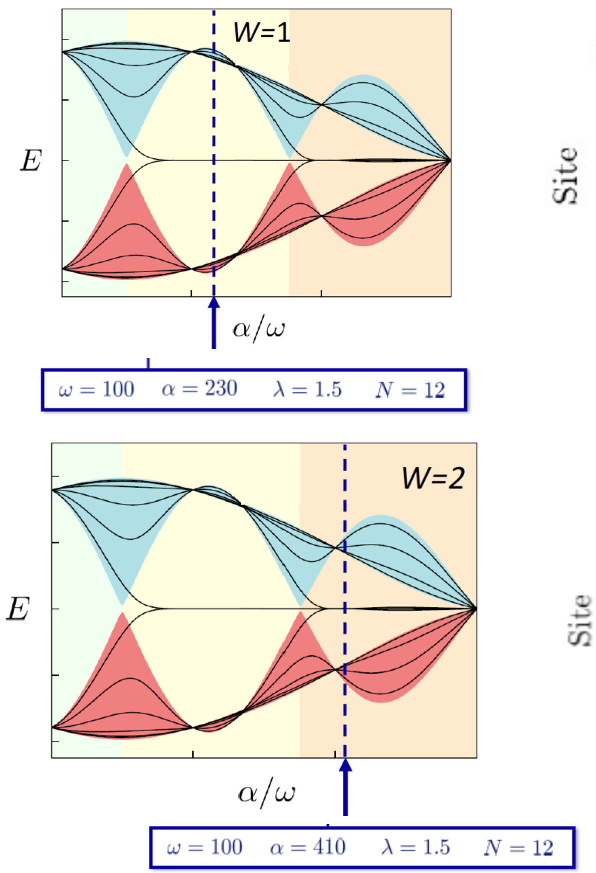

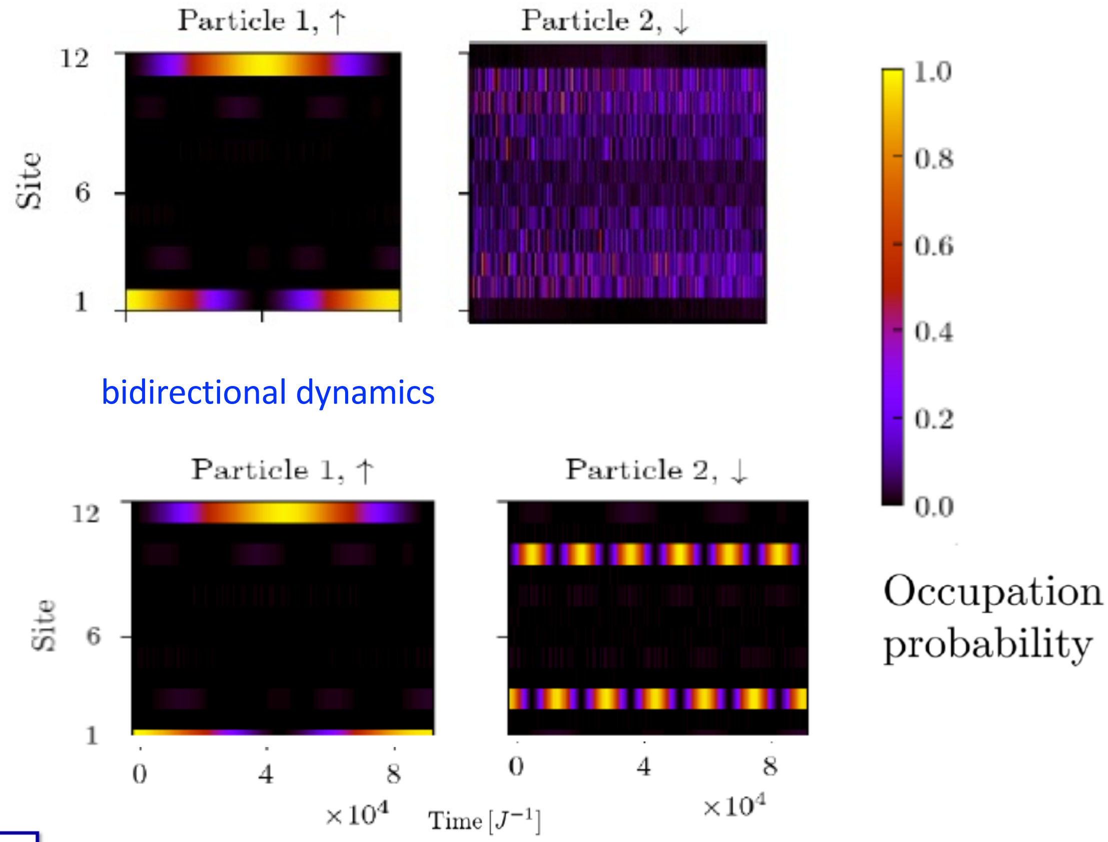

The transfer time depends on the edge states hybridization: slow dynamics

Control of the transfer

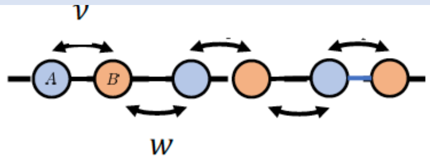

Decay length ∝ v/w

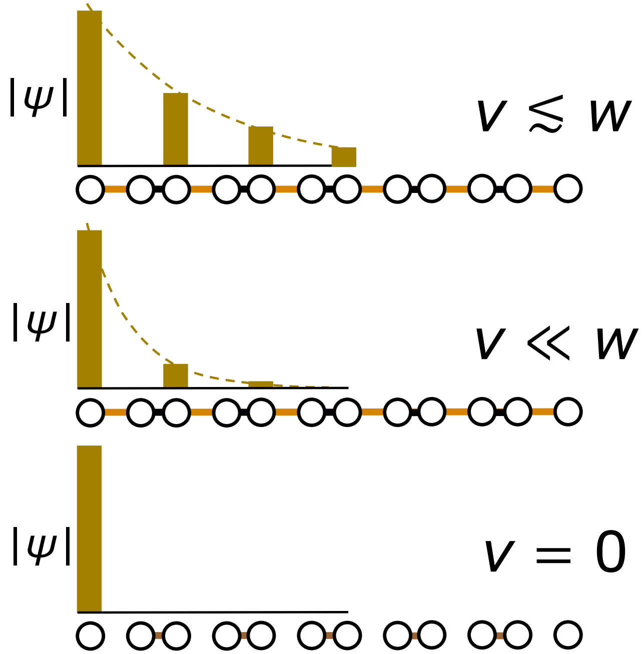

$L = 12,\ w = 1$

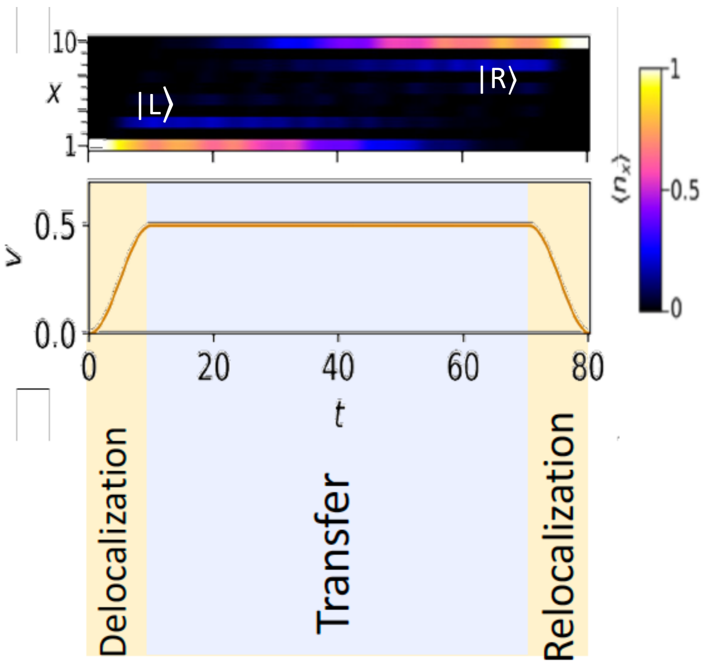

$$v(t) = \begin{cases} v_0 \sin^2(\Omega t) & \text{if } 0 \le t \le t_{\rm prep} \\ v_0 & \text{if } t_{\rm prep} < 0 \le t_{\rm tr} - t_{\rm prep} \\ v_0 \sin^2[\Omega(t - t_{\rm tr})] & \text{if } t_{\rm tr} - t_{\rm prep} < t \le t_{\rm tr}, \end{cases}$$

Transfer time

$$t_{tr} \propto e^{L/2}$$

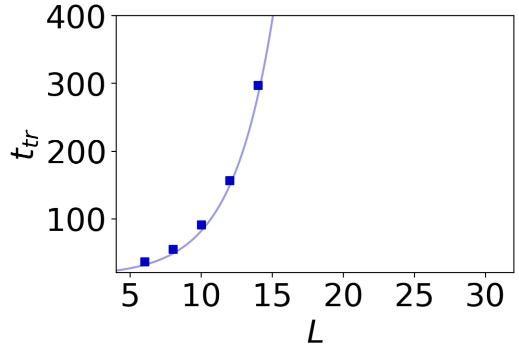

$$t_{tr} \propto (\langle \mathcal{L} | \mathcal{H} | \mathcal{R} \rangle)^{-1}$$

slow transfer

Problem: Transfer time scales exponentially with L

Can we add amplifiers?

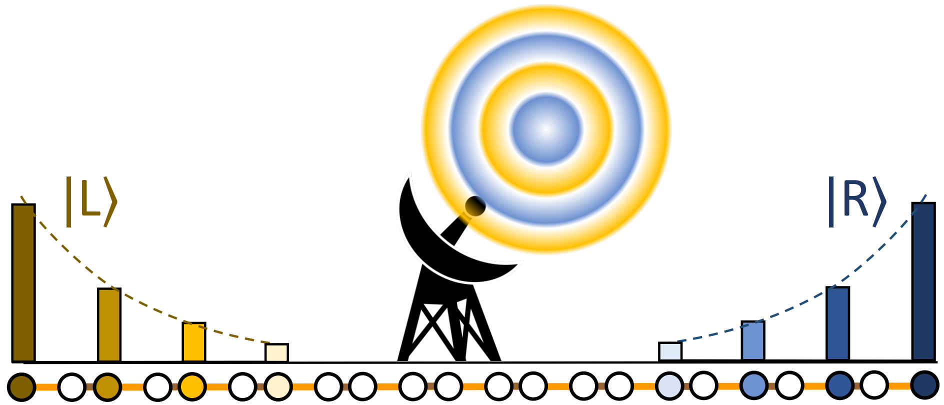

Topological domain walls as quantum amplifiers

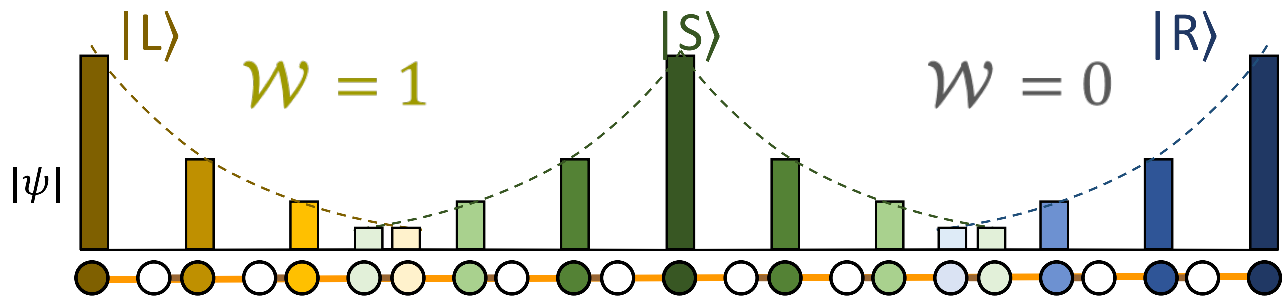

J. Zurita et al., Quantum 7, 1043 (2023)

L = 11
2 Domains

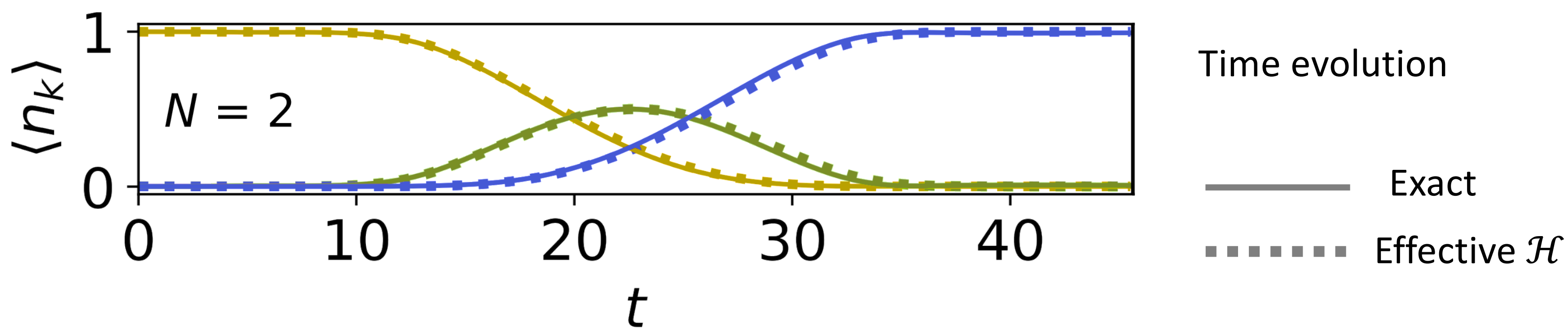

one, two and four-domains transfer time

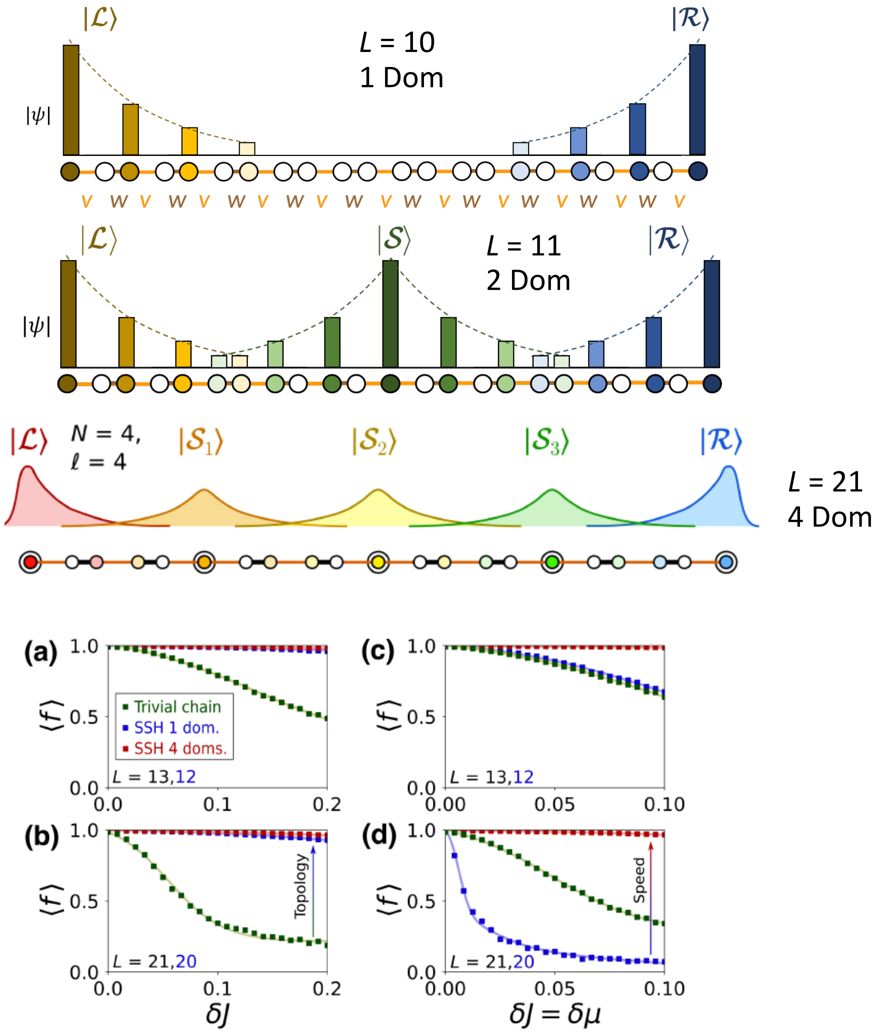

Off-diagonal disorder

Off-diagonal and diagonal disorder

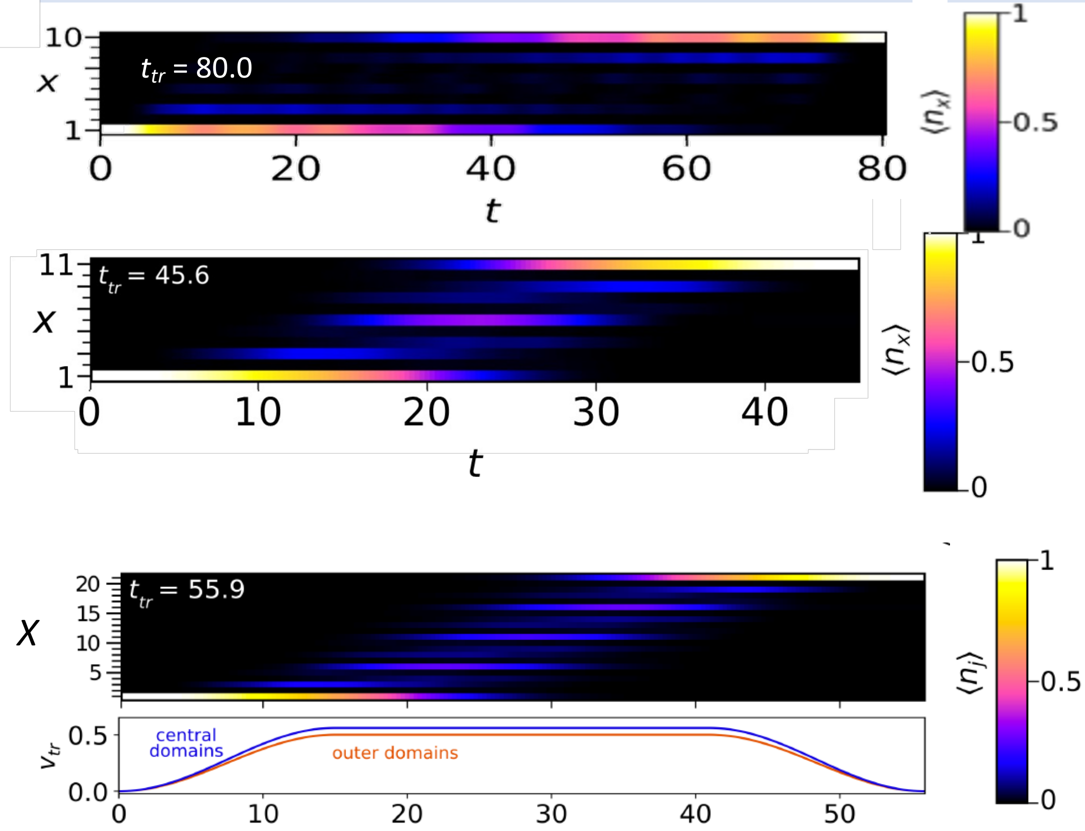

Topological domain walls as quantum amplifiers

Two-domain transfer: still exponential

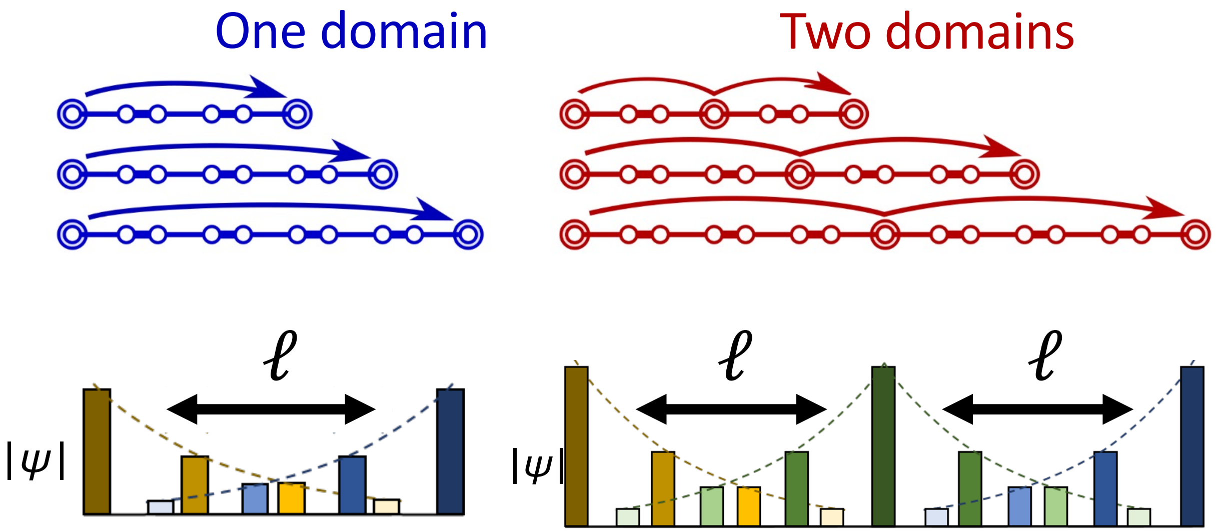

Transfer time depends exponentially
on domain length ℓ only

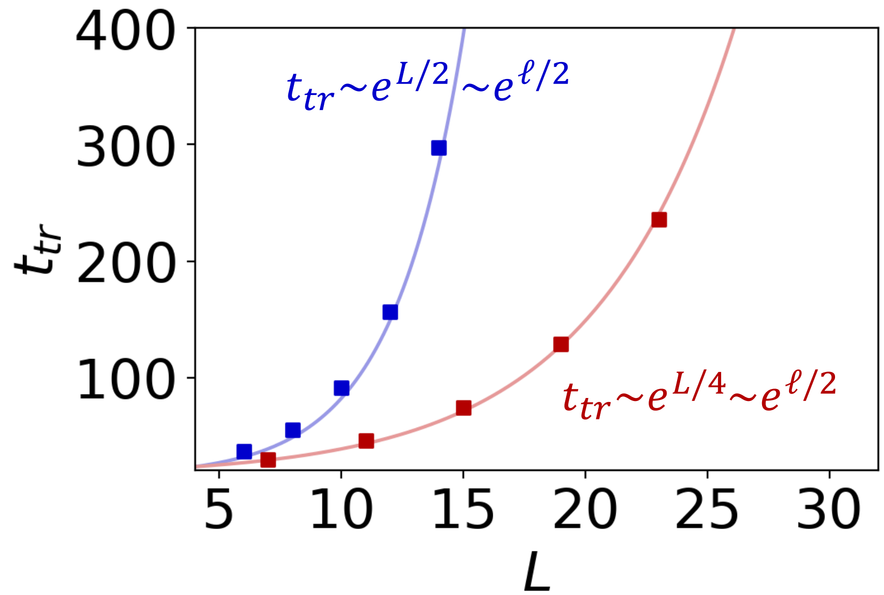

Topological domain walls as quantum amplifiers

Transfer time (L = 26):
1 dom: 1131.2 ns
5 doms: 4.1 ns

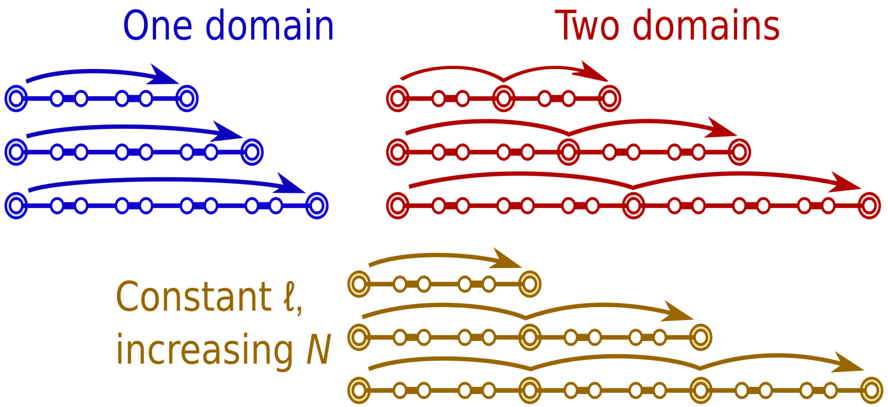

$$t_{tr} \sim e^{\ell/2}$$

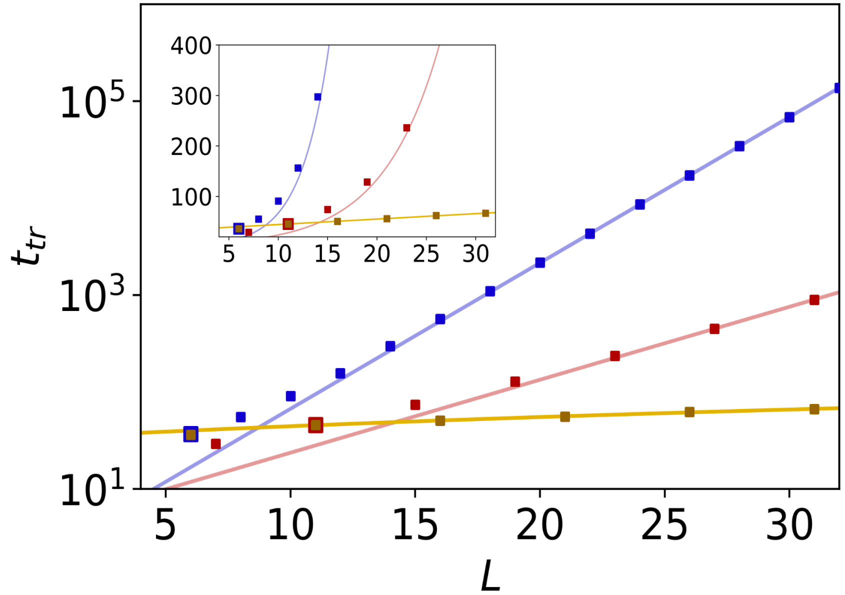

J. Zurita et al., Quantum 7, 1043 (2023)

Aharonov-Bohm caging

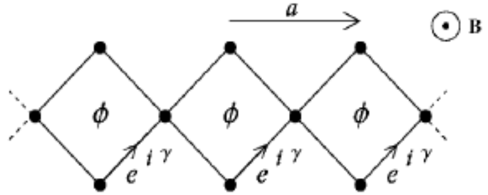

Vidal et al., PRL (1998)

When $\phi = \pi$, interference cancels the tunneling

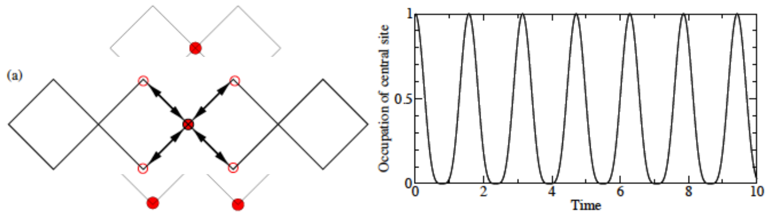

C.E. Creffield and G.Platero, PRL (2010)

Interaction-driven breakdown of Aharonov–Bohm caging in flat-band Rydberg lattices, T. Chen et al., Nature Phys. 2024

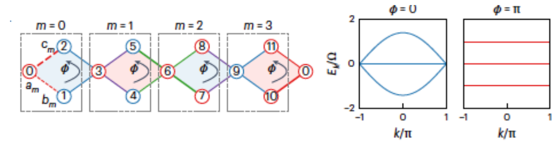

Aharonov-Bohm Caging and Inverse Anderson Transition in Ultracold Atoms, H. Li et al., PRL (2022)

AB-caging does not occur on every lattice –

- square, triangular, honeycomb – no caging
- Penrose, octagonal, $\mathcal{T}_3$ – caging possible

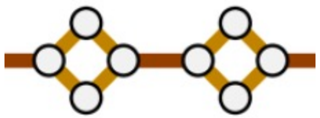

The diamond-necklace chain (DNC)

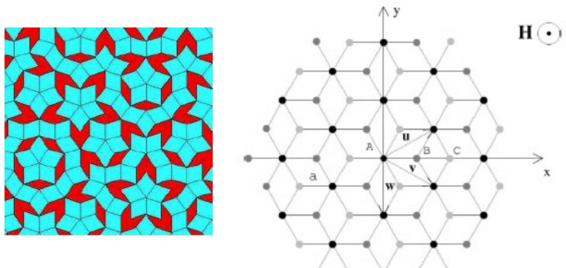

S. Mukherjee et al. PRL (2018)

AB caging has been observed in a variety of systems

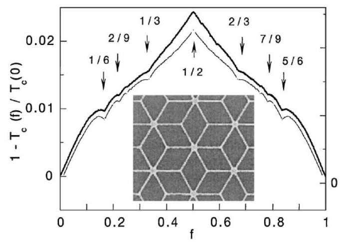

Aharonov-Bohm cage in a superconducting wire network

AB caging in a photonic lattice (rhombus chain)

Di Liberto et al. Phys Rev A (2019)

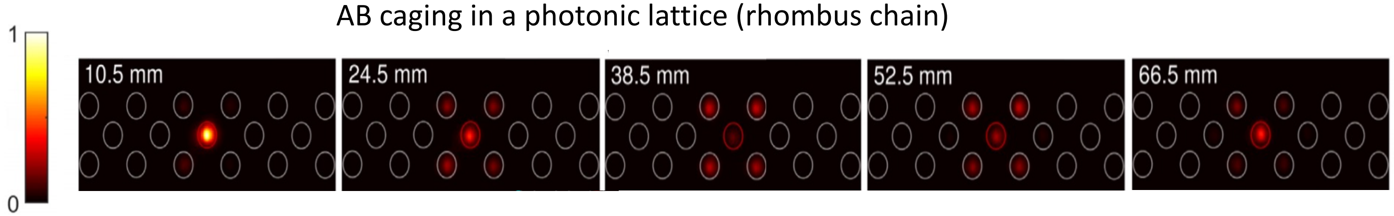

The Creutz Ladder

$$\mathcal{H}_C = -\sum_{\substack{j=1 \\ \alpha=A,B}}^{L-1} \left\{ J_\alpha c^\dagger_{j+1,\alpha} c_{j,\alpha} + J c^\dagger_{j+1,\bar{\alpha}} c_{j,\alpha} + h.c. \right\} - m \sum_{R=1,A}^{L,B} c^\dagger_{j,\alpha} c_{j,\bar{\alpha}}$$

$$\phi = \frac{q}{\hbar}\Phi \equiv 2\pi \frac{\Phi}{\Phi_0}$$

Magnetic flux

$$J_\alpha = J e^{i s_\alpha \phi/2} \qquad s_{A/B} = \pm 1$$

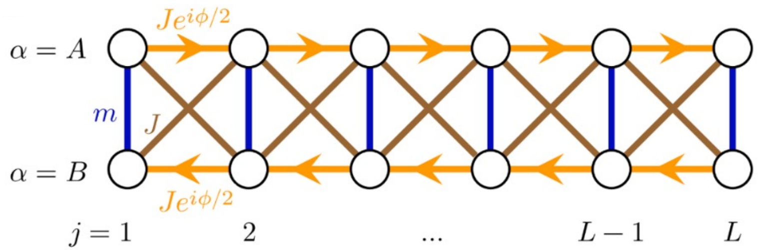

M. Creutz. Physical Review Letters (1999)

Aharonov-Bohm caging in the Creutz Ladder

$$\mathcal{H}_C = -\sum_{\substack{j=1\\ \alpha=A,B}}^{L-1}\left\{J_\alpha c^\dagger_{j+1,\alpha}c_{j,\alpha} + J c^\dagger_{j+1,\bar{\alpha}}c_{j,\alpha} + h.c.\right\} - m\sum_{R=1,A}^{L,B} c^\dagger_{j,\alpha}c_{j,\bar{\alpha}}$$

$$\phi = \frac{q}{\hbar}\Phi \equiv 2\pi\frac{\Phi}{\Phi_0}$$

Magnetic flux

$$J_\alpha = J e^{i s_\alpha \phi/2} \qquad s_{A/B} = \pm 1$$

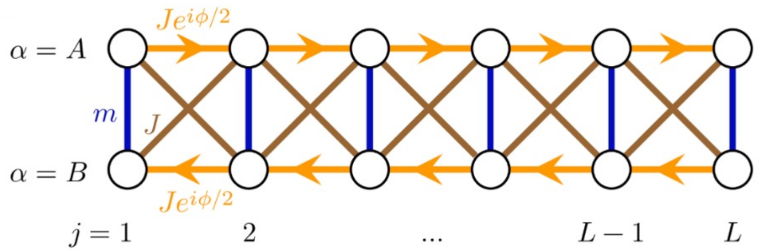

M. Creutz. Physical Review Letters (1999)

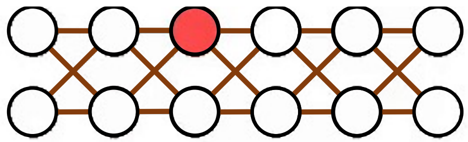

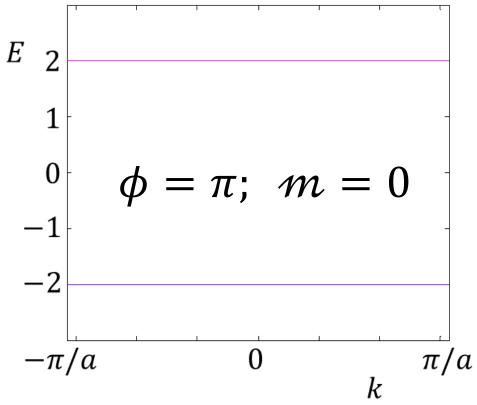

Flat bands

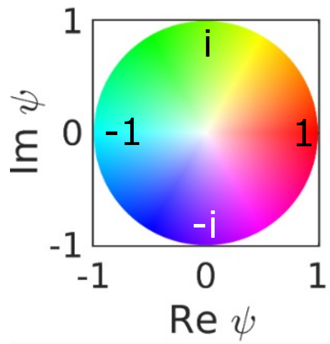

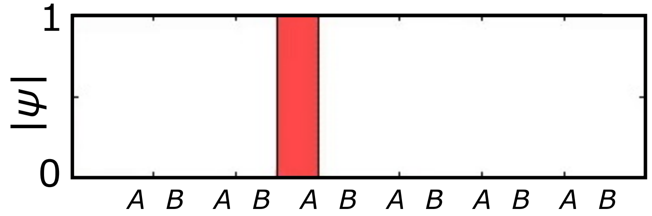

J=1

J. Zurita et al., Adv. Quantum Tech., 2019
J. Zurita et al., Quantum 2021

AB caging in the Creutz Ladder

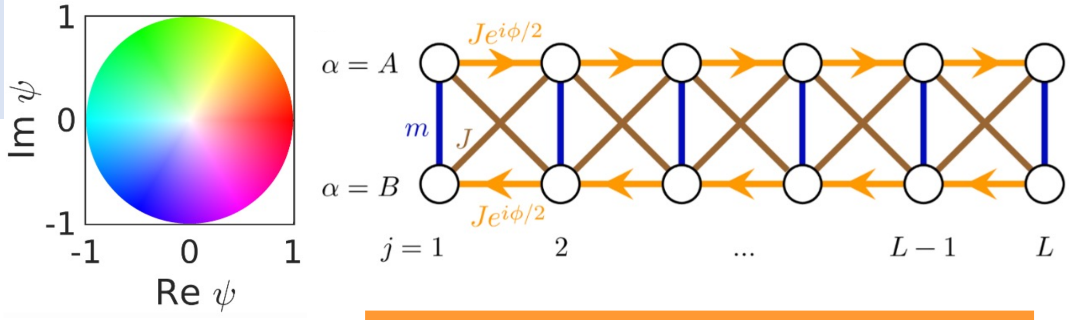

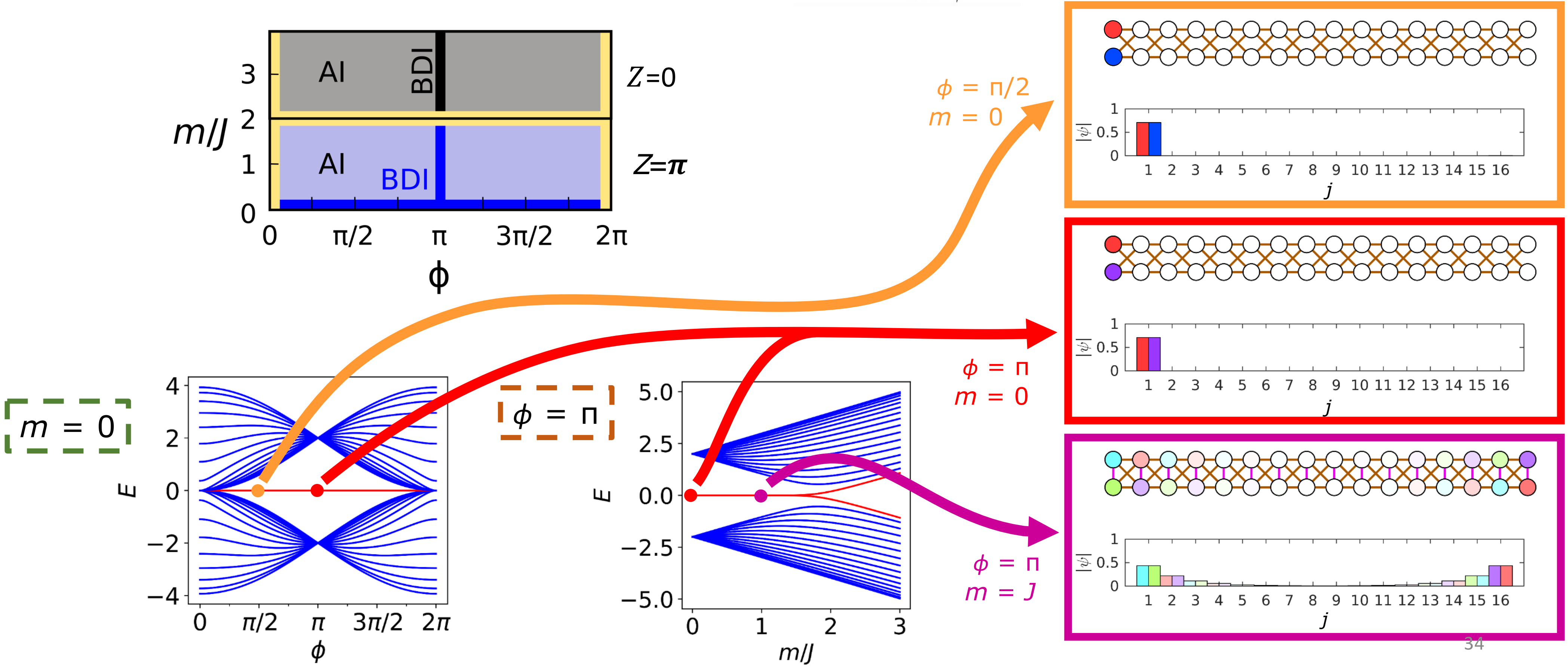

The Creutz Ladder: The two Chiral operators

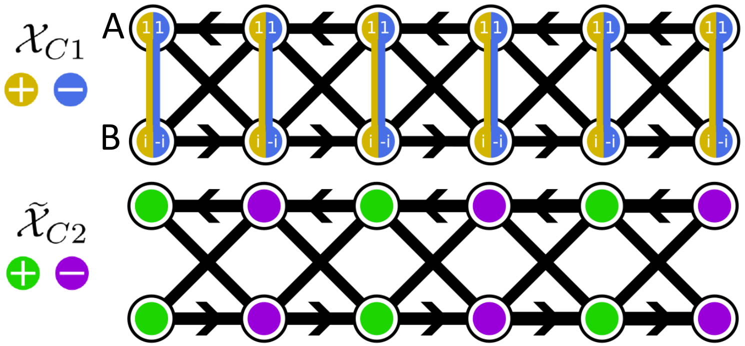

non-local chiral symmetry $X_{C1} = \sigma_y$ if $\phi = \pm\pi$, winding number $\nu = \pm 1$

X_{C1} is not diagonal: it does not protect against a general off-diagonal disorder

X_{C1} eigenstates: $|A\rangle \pm i|B\rangle$

Hidden chiral symmetry

$X_{C2} = \mathrm{diag}(1, 1, -1, -1)$ $\phi \neq 0 \bmod 2\pi$ Eigenstates: single-site states $|j, \alpha\rangle$, with their chirality being $(-1)^{j+1}$

X_{C2} explains the protection against off-diagonal disorder of the π- flux CL end modes, which cannot be explained using standard symmetries.

Hidden: they do not have the periodicity of the lattice

Hidden Symmetries are symmetries of H that do not conmute with the lattice translations

The Creutz Ladder: The two Chiral operators

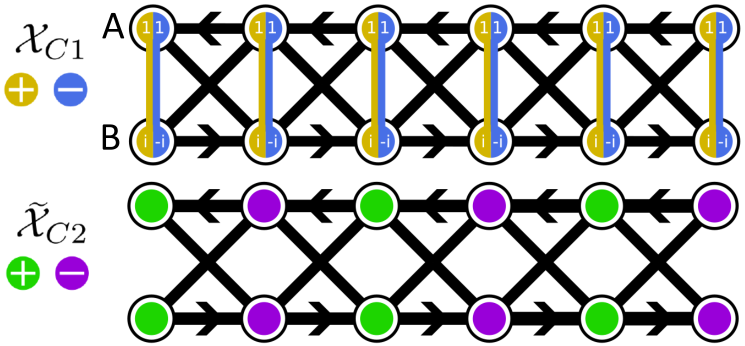

non-local chiral symmetry $X_{C1} = \sigma_y$ if $\phi = \pm\pi$, winding number $\nu = \pm 1$

X_{C1} is not diagonal: it does not protect against a general off-diagonal disorder

X_{C1} eigenstates: $|A\rangle \pm i|B\rangle$

Hidden chiral symmetry

$X_{C2} = \mathrm{diag}(1, 1, -1, -1)$ $\phi \neq 0 \bmod 2\pi$ Eigenstates: single-site states $|j, \alpha\rangle$, with their chirality being $(-1)^{j+1}$

X_{C2} explains the protection against off-diagonal disorder of the π- flux CL end modes, which cannot be explained using standard symmetries.

Hidden: they do not have the periodicity of the lattice

$(\phi, m, \epsilon, r) = (\pi/2, 0, 0, 1)$

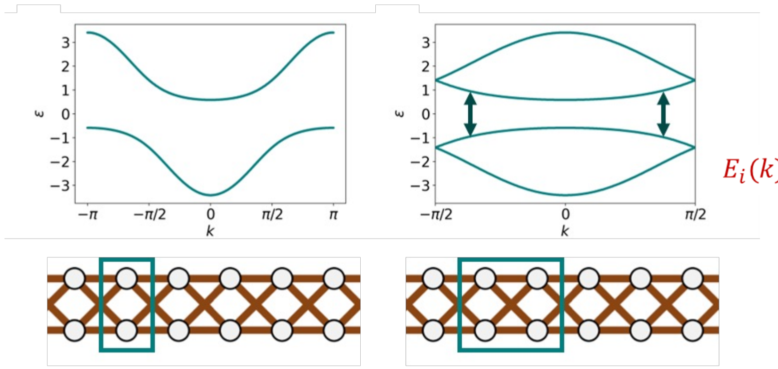

$E_i(k) = -E_j(k)$

2-site unit cell: no manifest chiral symmetry

4-site unit cell: chiral symmetry appears

$\tilde{k} = 2k$ four-site cell momentum

$$\tilde{\mathcal{H}}(k) = \begin{pmatrix} 0 & \tilde{h}(\tilde{k}) \\ \tilde{h}(\tilde{k})^\dagger & 0 \end{pmatrix} \qquad \tilde{h}(\tilde{k}) = -2Je^{-i\tilde{k}/2} \begin{pmatrix} \cos\frac{\phi-\tilde{k}}{2} & r\cos\frac{\tilde{k}}{2} \\ r\cos\frac{\tilde{k}}{2} & \cos\frac{\phi+\tilde{k}}{2} \end{pmatrix}$$

J. Zurita et al., Phys. Rev. B, 111, 155406 (2025)

The Creutz Ladder: The two chiral operators

(ϕ, r, ϵ)

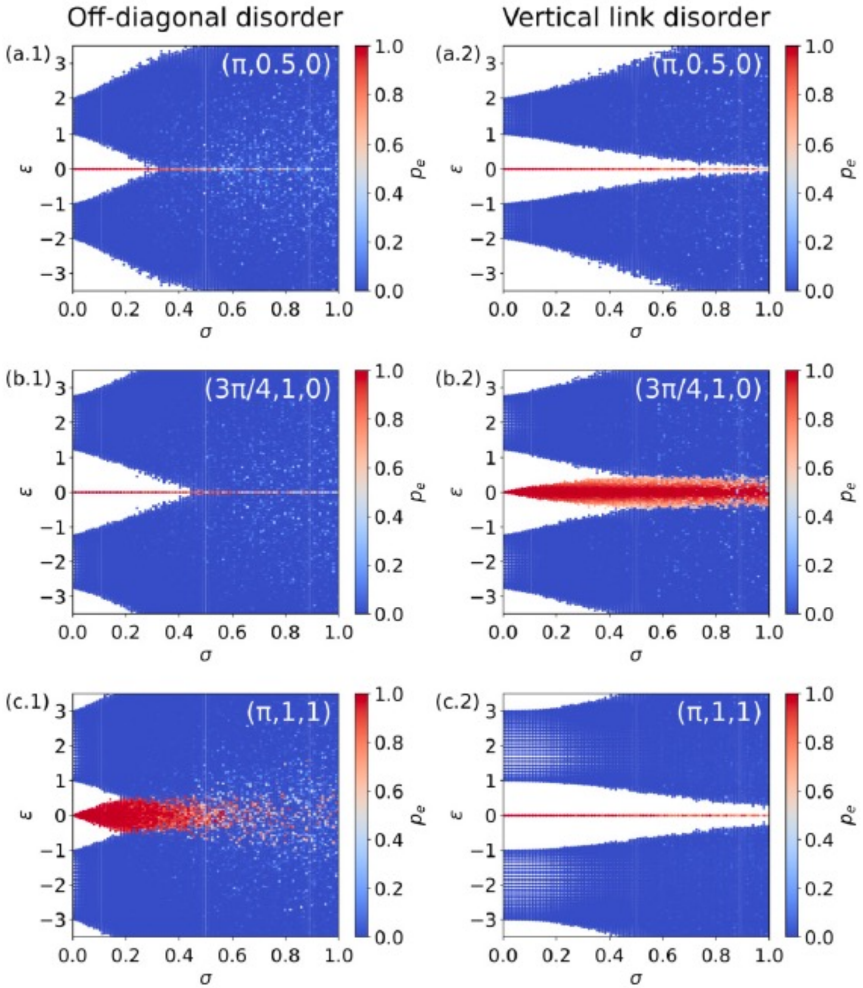

The double chiral region

$$(\phi = \pm\pi\,,\, r)$$

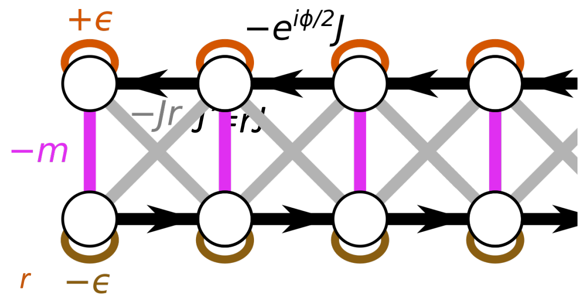

$\mathcal{X}_{C1}$ broken

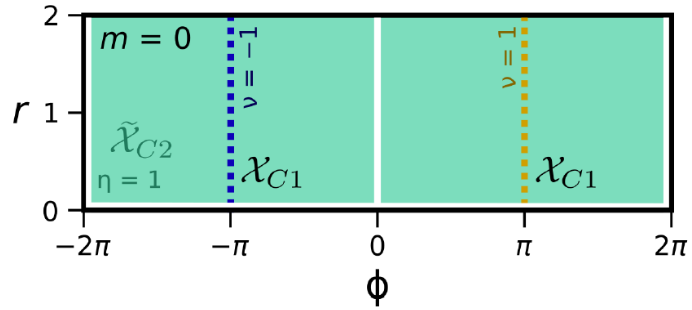

$\tilde{\mathcal{X}}_{C2}$ broken

J. Zurita, C. Creffield, G. Platero,
Phys. Rev. B **111**, 155406 (2025)

Topological Domain walls in the Creutz Ladder

The magnetic Peierls phases ϕ_j can be used to define different domains.

Each DW hold two protected states: it is possible to decouple one, such that its partner can leapfrog over it without disturbing intermediate states

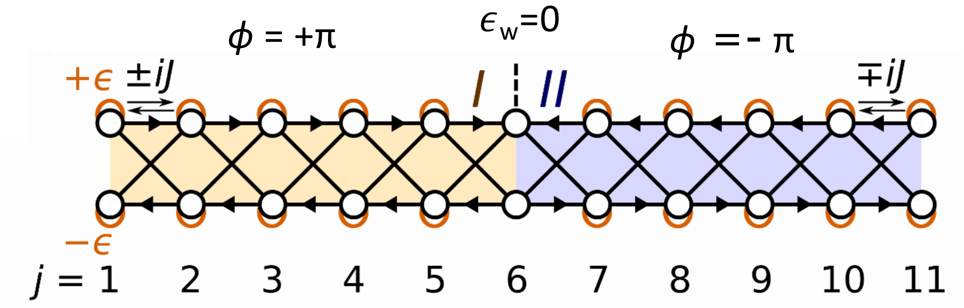

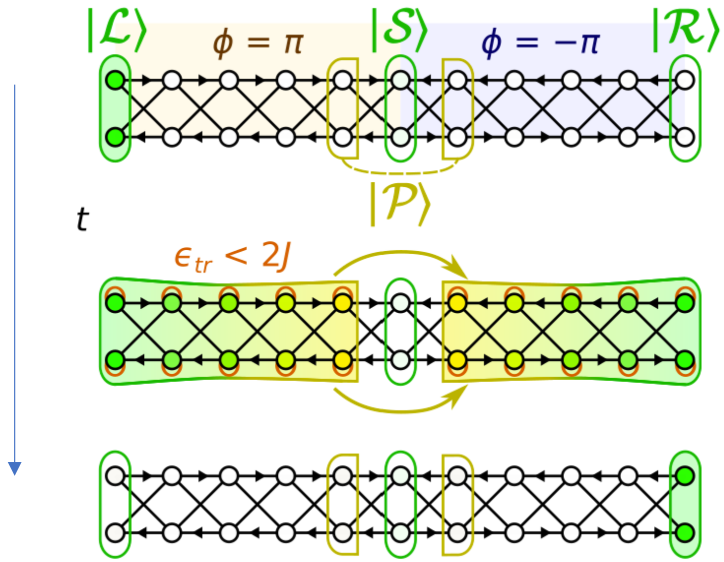

The domain wall has $|\nu 2 - \nu 1| = 2$ zero modes (v = +-1)

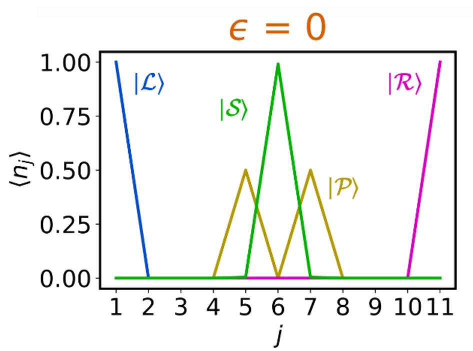

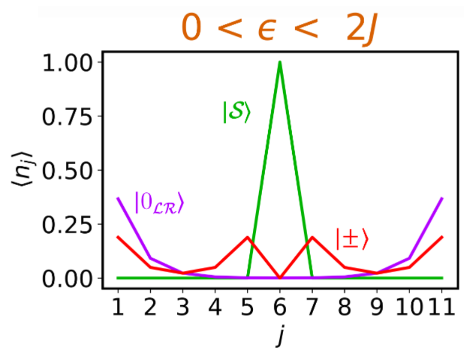

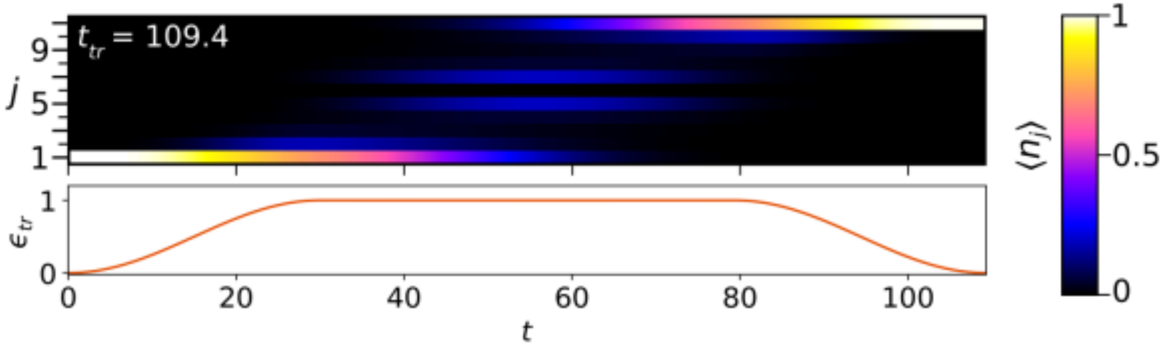

J. Zurita et al., Quantum 7, 1043 (2023)

One of them can be kept isolated

Topological Domain walls in the Creutz Ladder

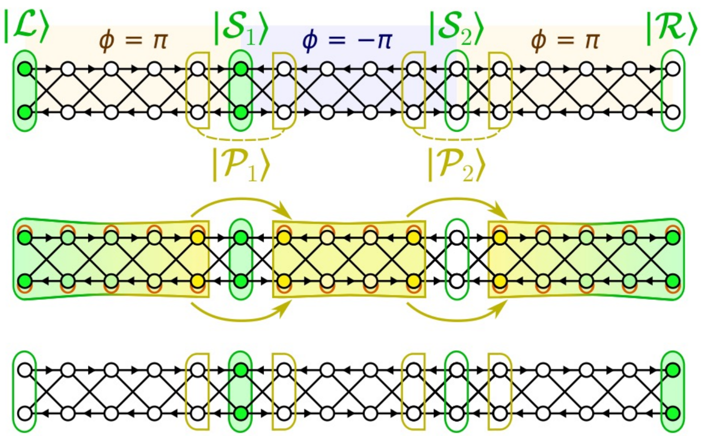

.....without disturbing intermediate states

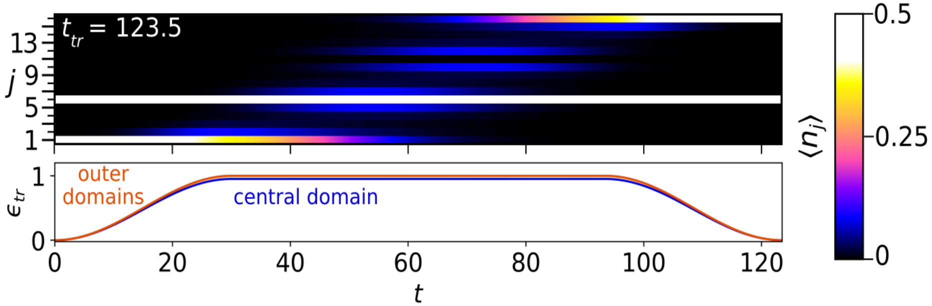

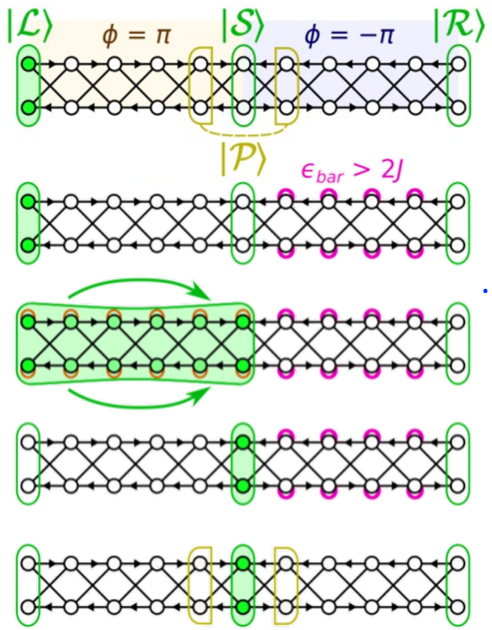

...and can also involve domain walls

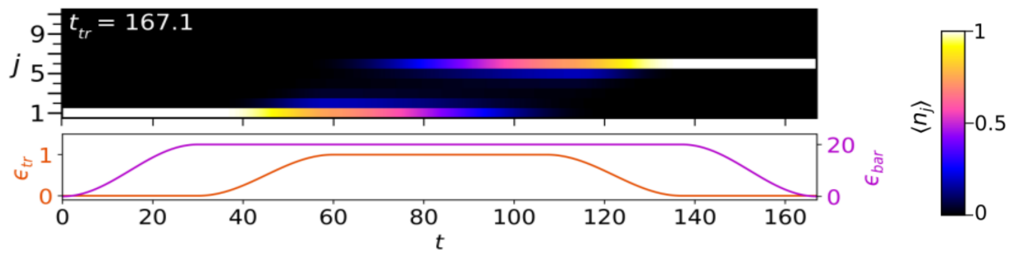

J. Zurita et al., Quantum 7, 1043 (2023)

From Topology to Qubits

If we associate:

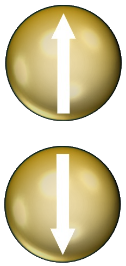

$|0\rangle_L \leftrightarrow$

$|1\rangle_L \leftrightarrow$

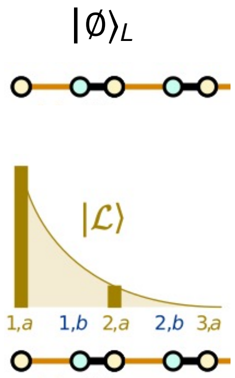

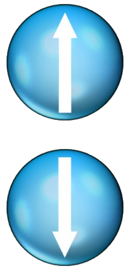

$|0\rangle_R \leftrightarrow$

$|1\rangle_R \leftrightarrow$

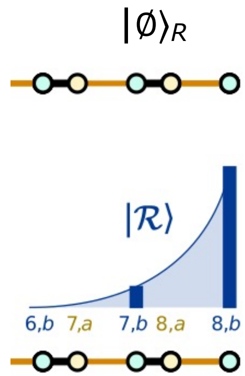

...we can entangle distant qubits using $|\pm\rangle$!

Qubits in an SSH structure

[4] F. Mei et al., Phys. Rev. A **98**, 012331 (2018)

Qubits coupled to an SSH chain

[2] N. Lang, H. P. Büchler. npj Quantum Inf. **3**, 47 (2017)

[5] M. Bello et al., Sci. Adv. **5**, eaaw0297 (2019)

Application: entanglement distribution with DWs

Experimental proposal: qubit-cavity couplings

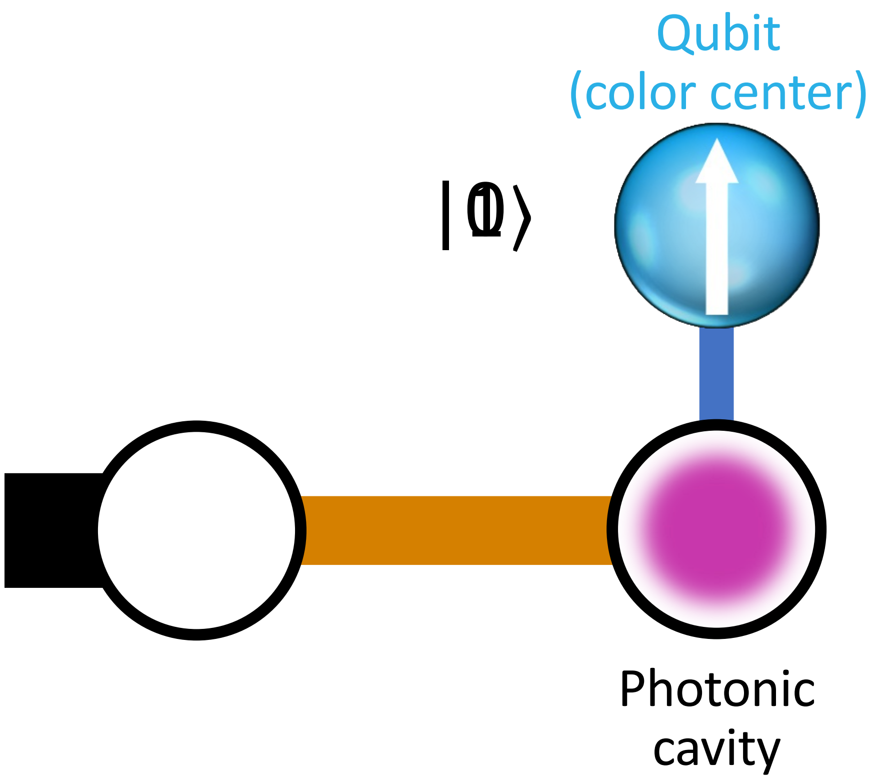

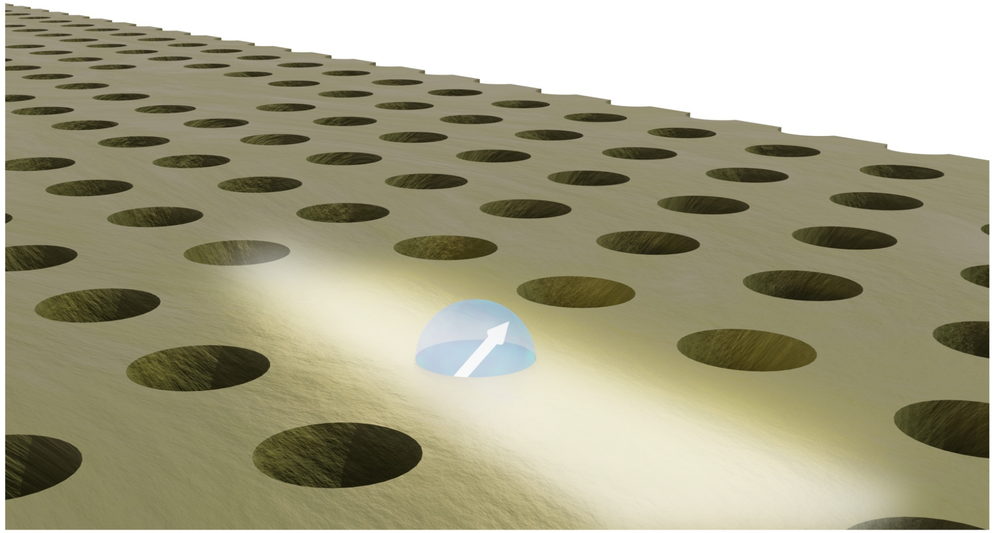

Shown experimentally [2]
in this platform

[1] Hollenbach et al., Optics Express **28**, 26111 (2020)
[2] Baron et al., Appl. Phys. Lett. **121**, 084003 (2022)
[3] J. Zurita, A. Agustí Casado, C. Creffield, G. Platero, Quantum **9**, 1625 (2025)

Application: entanglement distribution with DWs

Topological photonic lattice coupled to color center emitters

Hollenbach et al., Optics Express (2020)
Baron et al., Appl. Phys. Lett. (2022)
Redgem et al., Nature Comm., (2023)

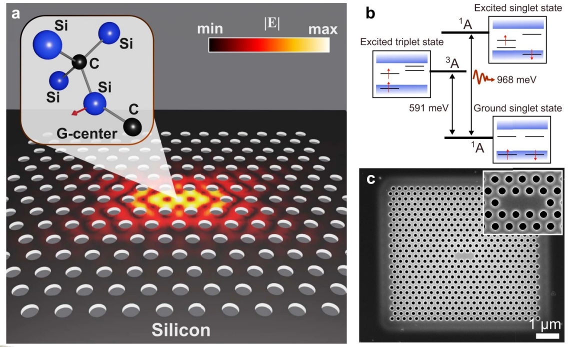

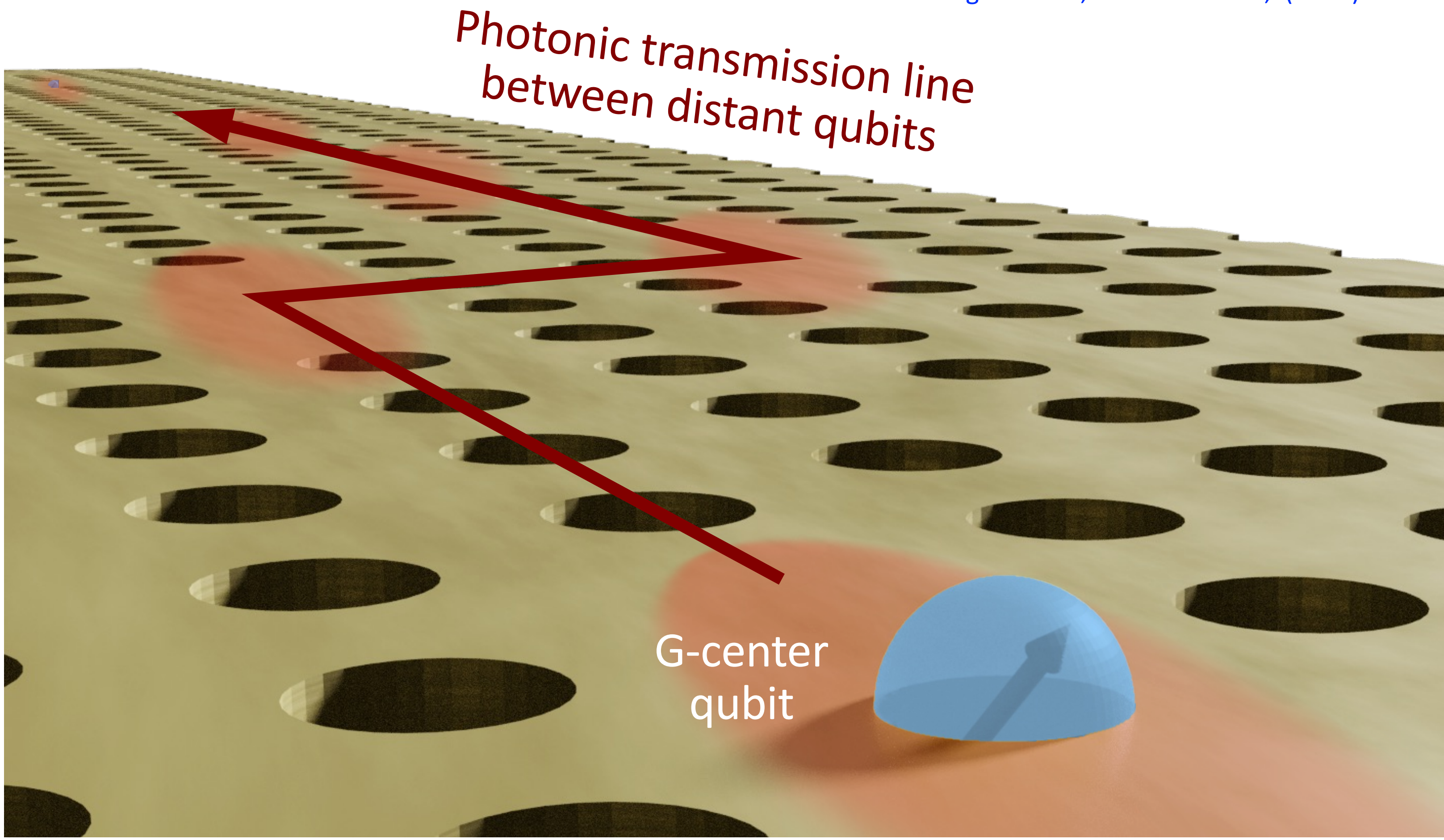

Application: entanglement distribution with DWs

The stub-SSH (SSSH) model

N domains : 2N boundary states protected against off-diagonal disorder if: w> v, u

- u_k connect the cavities at the ends and the stubs to the rest
- Alternating winding numbers: 1 and -1.

- Two chiral states: *S* and *P* located at each wall
- *S* states interface with the qubit
- *P* states used for the transfer

l=4 cavities per domain

N=4 domains

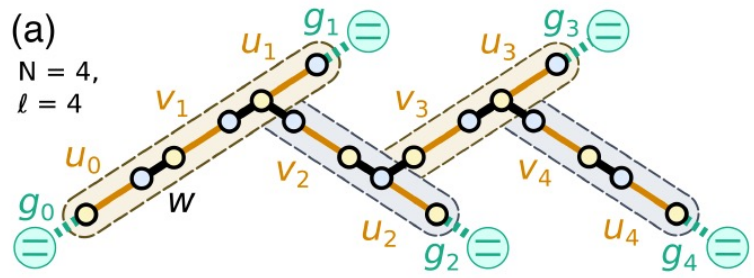

1) Transfer process between the two ends

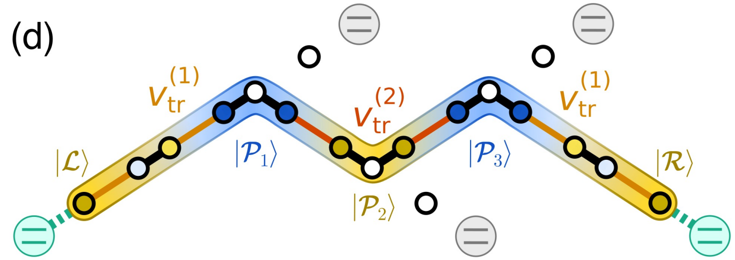

2) Transfer process between the left end and the first wall

$v_{\mathrm{tr}} < w$

$v_{\mathrm{bar}} \gg w$ stops it.

P dissappears for v_{bar}>w

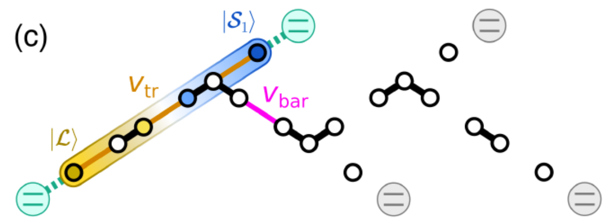

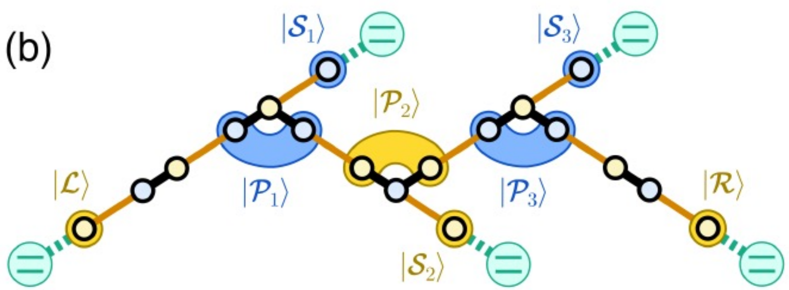

J. Zurita et al., Quantum, **9**, 1625 (2025)

Preparing a Bell state between arbitrary pairs of qubits

Photon transfer through the topological lattice

Ground and excited states of the qubit L $|0\rangle_L$ and $|1\rangle_L$ The vacuum state of the photonic lattice $|\varnothing\rangle_\gamma$

i) Prepare the initial state $|1\rangle_L \otimes |0\rangle_R \otimes |\varnothing\rangle_\gamma$ ii) Execute a $(\Pi/2)_{01}^{(L)}$ Operation between the qubit L and its cavity

iii) Full transfer T_{LR} of the photonic amplitude to the right most cavity   iv) Execute a second π pulse on g_R:

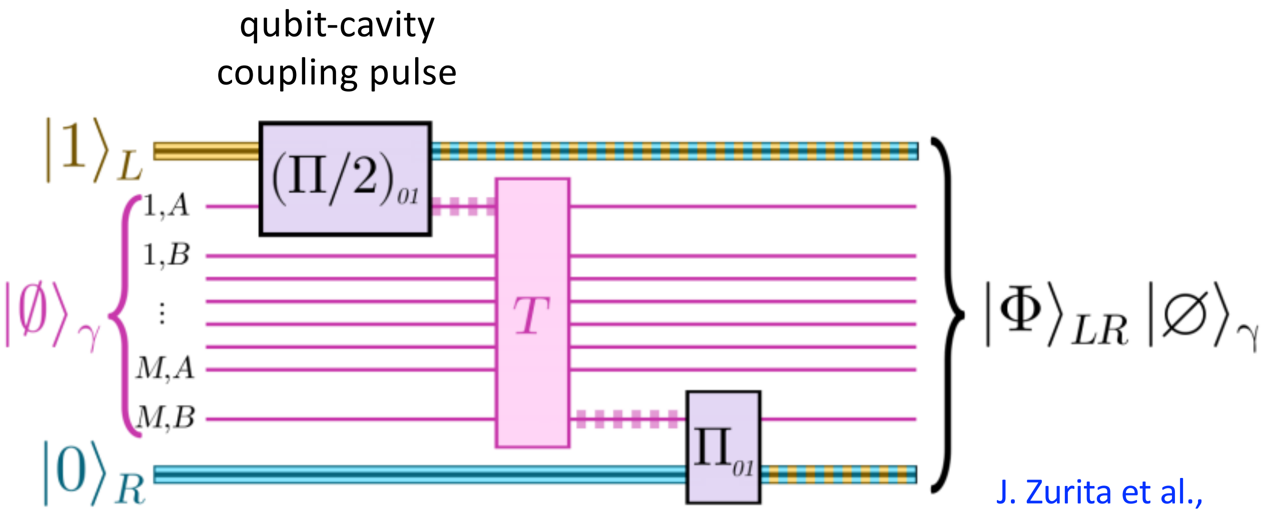

J. Zurita et al.,
Quantum, **9**, 1625 (2025)

$$\boxed{|\Phi\rangle_{LR} = \frac{1}{\sqrt{2}}\left[|10\rangle + e^{i\theta}\,|01\rangle\right]}$$

$$e^{i\theta} = [(-1)^{\ell/2+1} i]^{n_d}$$

n_d total number of domains

ℓ number of sites per domain

Application: entanglement distribution with DWs

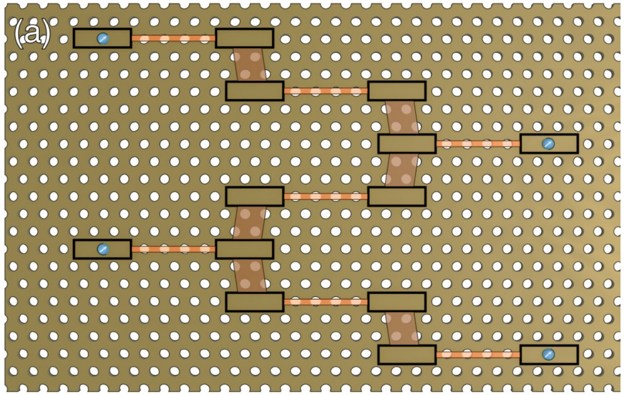

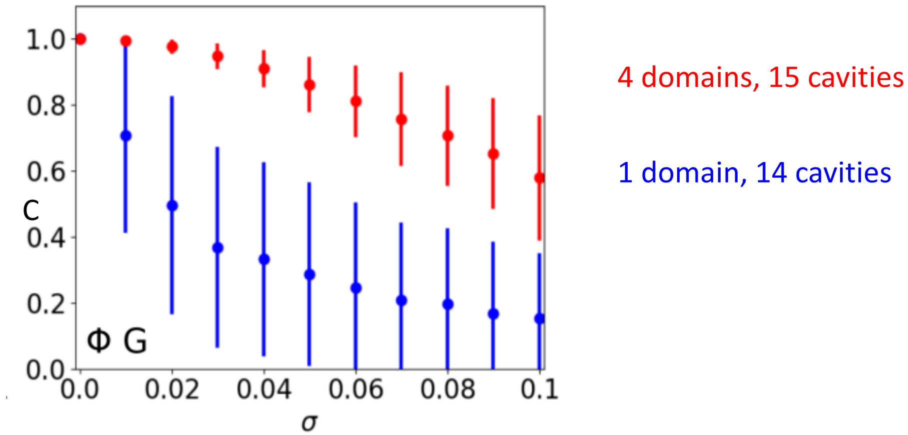

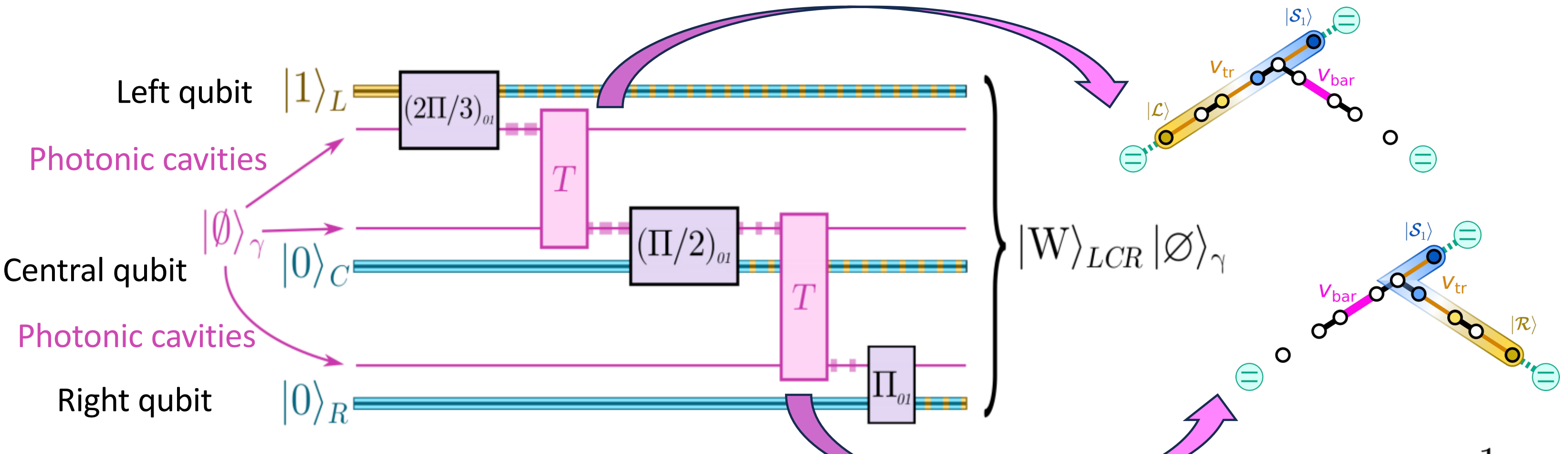

$$|\mathrm{W}\rangle_{LCR} = \frac{1}{\sqrt{3}}\left[|100\rangle - i\,|010\rangle + |001\rangle\right]$$

J. Zurita et al., Quantum, **9**, 1625 (2025)

Square rooth Topological Insulators

- Rhombus chain: 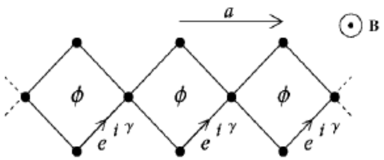

H^2 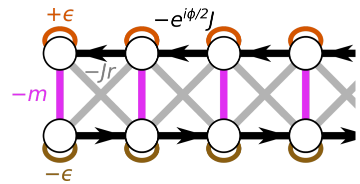

- The necklace chain: 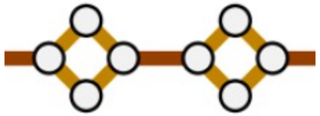

hidden chiral symmetry: $\tilde{X}_{\diamond} = \mathrm{diag}_8(1, -1, -1, 1, -1, 1, 1, -1)$

Conclusions

- Topological Edge States can be implemented in different platforms, they allow the transfer of quantum information with high fidelity
- The use of topological domain walls can significatively speed-up the transfer of quantum information
- Domain walls with two states can be used to create quasi-1D networks with full connectivity
- The quantum transfer through a topological lattice can be used to generate entanglement between distant qubits

J. Zurita et al., Quantum 7, 1043 (2023); Phys. Rev. B, 111, 155406 (2025); Quantum, 9, 1625 (2025)

Acknowledgement to my collaborators

Quantum state transfer through edge states and Topological Domain Walls

Juan Zurita, ICMM-CSIC   **Charles Creffield** UCM

Floquet engineering to simulate the extended SSH and topological edge states in a QD array

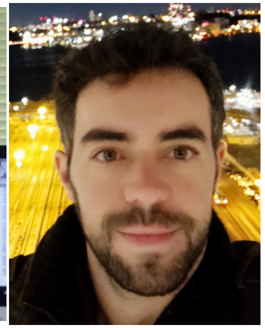

Beatriz Pérez
Augsburg University

Miguel Bello
IFIMAC, UAM

Álvaro Gómez Léon
IFF (CSIC)

Spin qubits in QD arrays, quantum control

David Fernández
ICMM-CSIC

Xi Chen
ICMM-CSIC

Yue Ban
ICMM-CSIC

Thank you for your attention!